ONLINE AND OFFLINE MEASUREMENT OF TOTAL SOLUBLE SOLIDS IN MANGO (*MANGIFERA INDICA* L. CV NAMDOKMAI SITHONG) USING NEAR INFRARED SPECTROSCOPY

SNEHA SHARMA

A THESIS SUBMITTED IN PARTIAL FULFILLMENT

OF THE REQUIREMENT FOR THE DEGREE OF

MASTER OF ENGINEERING IN AGRICULTURAL ENGINEERING

FACULTY OF ENGINEERING

KING MONGKUT'S INSTITUTE OF TECHNOLOGY LADKRABANG

2018

KMITL-2018-EN-M-100-174

ONLINE AND OFFLINE MEASUREMENT OF TOTAL SOLUBLE SOLIDS IN MANGO (*MANGIFERA INDICA* L. CV NAMDOKMAI SITHONG) USING NEAR INFRARED SPECTROSCOPY

SNEHA SHARMA

A THESIS SUBMITTED IN PARTIAL FULFILLMENT
OF THE REQUIREMENT FOR THE DEGREE OF
MASTER OF ENGINEERING IN AGRICULTURAL ENGINEERING
FACULTY OF ENGINEERING
KING MONGKUT'S INSTITUTE OF TECHNOLOGY LADKRABANG
2018

KMITL-2018-EN-M-100-174

หัวข้อวิทยานิพนธ์	การวัดปริมาณของแข็งที่ละลายน้ำได้ของมะม่วงพันธุ์น้ำดอกไม้สีทองแบบออนไลน์และออฟไลน์ด้วยเนียร์อินฟราเรดสเปกโทรสโกปี
นักศึกษา	Ms. Sneha Sharma
รหัสประจำตัว	59601330
ปริญญา	วิศวกรรมศาสตรมหาบัณฑิต
สาขาวิชา	วิศวกรรมเกษตร
พ.ศ.	2561
อาจารย์ที่ปรึกษาวิทยานิพนธ์	รศ.ดร.ปานมนัส ศิริสมบูรณ์

บทคัดย่อ

ความแม่นยำของเครื่องวัดแบบเนียร์อินฟราเรดสเปกโทรสโกปีที่ใช้สำหรับวัดปริมาณของแข็งที่ละลายน้ำได้ของมะม่วงถูกวัดโดยการคำนวณค่าการทวนซ้ำและการทำซ้ำ ซึ่งการวัดครั้งนี้ใช้สเปกโตรมิเตอร์แบบ Short wave UV-Vis-NIR fiber optic diode array และ whole NIR range Fourier Transform (FT) NIR สภาวะการวัดแบบออนไลน์และออฟไลน์ได้ถูกประยุกต์ในการวัดความแม่นยำของเครื่องสเปกโตรมิเตอร์แบบ Fiber optic diode array ถูกใช้สำหรับสภาวะออนไลน์ ส่วนสเปกโตรมิเตอร์แบบ FT-NIR ถูกใช้ในการวัดแบบออฟไลน์ พบว่าค่าการทวนซ้ำและการทำซ้ำในการสแกนแบบออฟไลน์มีค่าต่ำคือ 0.000775 และ 0.008262 เมื่อเปรียบเทียบกับแบบออนไลน์ 0.00419 และ 0.032041 ความแม่นยำของการวัดค่าอ้างอิงของปริมาณของแข็งที่ละลายน้ำได้ของมะม่วงถูกพิจารณาโดยการคำนวณค่าทวนซ้ำและค่าสัมประสิทธิ์การพิจารณาสูงสุด ความคลาดเคลื่อนจากวิธีอ้างอิงเท่ากับ 3.3% และความถูกต้องเท่ากับ 96.7%.

สำหรับการวัดแบบออนไลน์ใช้สเปกโตรมิเตอร์แบบ AvaSpec 2048 standard fiber optic spectrometer (short wave 200-1100 nm) ส่วนการวัดแบบออฟไลน์ใช้ MPA FT-NIR spectrometer (full wave 800-2500 nm) จำนวนตัวอย่างทั้งหมดสำหรับการสร้างแบบจำลองหลังจากที่จัดการสเปกตรัมผิดปกติเท่ากับ 182 ช่วงของปริมาณของแข็งที่ละลายน้ำได้ของมะม่วงในงานวิจัยนี้อยู่ระหว่าง 14-20% การสร้างแบบจำลองของทั้งสองสภาวะใช้วิธี Partial least square (PLS) regression สัมประสิทธิ์การพิจารณา (R^2) และค่ารากที่สองของความคลาดเคลื่อนยกกำลังสองเฉลี่ยของการประมาณ (RMSEE) ของแบบจำลองที่เหมาะสมของแบบการสแกนแบบออฟไลน์เท่ากับ 0.70 และ 0.729% โดยมี PLS factor เท่ากับ 8 สำหรับการสแกนแบบออนไลน์ค่า R^2 และค่ารากที่สองของความคลาดเคลื่อนยกกำลังสองเฉลี่ยของการสร้างแบบจำลอง (RMSEC) เท่ากับ 0.61 และ 0.726% โดยมี PLS factor เท่ากับ 6 แบบจำลองเหล่านี้ถูกนำมาใช้วัดปริมาณของแข็งที่ละลายน้ำได้ของชุดตัวอย่างใหม่ ซึ่งได้ค่าความคลาดเคลื่อนมาตรฐานของการทำนาย (SEP) ค่าความคลาดเคลื่อนเฉลี่ยลัอัตราส่วนของความเบี่ยงเบนในการทำนาย (RPD) ของชุดตัวอย่างใหม่โดยใช้แบบจำลองข้างต้นสำหรับการสแกนแบบแอดไลน์เท่ากับ 0.97%, -1.57% และ 1.27 ตามลำดับ ชุดตัวอย่างใหม่ที่ถูกสแกนโดยใช้ระบบสายพานร่วมกับชุดคัดแยกปริมาณของแข็งที่ละลายน้ำได้ สำหรับพิสูจน์แบบจำลองให้ค่า SEP ค่าความคลาดเคลื่อนเฉลี่ยและ RPD เท่ากับ 1.24%, -1.04% และ 1.02.

Thesis title	Online and Offline Measurement of Total Soluble Solids in Mango (*Mangifera Indica* L. CV Namdokmai Sithong) using Near Infrared Spectroscopy
Student	Ms. Sneha Sharma
Student ID.	59601330
Degree	Master of Engineering
Program	Agricultural Engineering
Year	2018
Thesis Advisor	Assoc. Prof. Dr. Panmanas Sirisomboon

ABSTRACT

The precision of Near Infrared (NIR) spectroscopic instrument used for measuring the total soluble solids (TSS) content of mango was measured by calculating the repeatability and reproducibility. Short wave UV-Vis-NIR fiber optic diode array spectrometer and whole NIR range Fourier Transform (FT) NIR spectrometer was used for the measurement. Online and offline condition was applied to measure the precision of the instrument. Fiber optic diode array spectrometer was used for the online measurement condition and FT-NIR spectrometer was used for the offline measurement condition. It was observed that the repeatability and reproducibility of offline scanning is low, 0.000775 and 0.008262 compared to the value obtained for online scanning 0.00419 and 0.032041, respectively. The precision of reference method to measure the TSS of mango was determined by calculating the repeatability and maximum coefficient of determination (R^2_{MAX}). The error from reference method was found to be 3.3% and with the accuracy value of 96.7%.

For the online measurement AvaSpec 2048 standard fiber optic spectrometer (short wave 200-1100 nm) was used. Offline scanning was done using the MPA FT-NIR spectrometer (full wave 800-2500 nm). Total number of sample used for model development after removing the outlier was 182. The TSS content of mango measured in this research was in the range of 14-20%. Partial least squares (PLS) regression was applied to develop the model for both conditions. The coefficient of determination (R^2) and root mean square error of estimation (RMSEE) of the optimum model of offline scanning was 0.70 and 0.729% with the PLS factor of 8. Similarly, for the online scanning R^2 and root mean square error of calibration (RMSEC) was obtained to be 0.61 and 0.726% with the PLS factor of 6. The model was further used to measure the TSS content of unknown sample set. The standard error of prediction (SEP), bias and ratio of predictive deviation (RPD) of the unknown set using the optimum model from offline scanning condition was 0.97%, 1.57% and 1.27

respectively. The unknown set of sample was scanned using the conveying system equipped with the mango sorting system for validating the model obtained by online scanning. The SEP, bias and RPD obtained were 1.24%, -1.06% and 1.02.

Acknowledgements

I would like to express my gratitude to my advisor Associate Professor Dr. Panmanas Sirisomboon for her exemplary advice, support and guidance throughout this study period. Without her support and advice, it would not be possible to achieve this success in my research and study. Her role throughout my research is an example of a great mentor.

I would like to acknowledge my family, for there consistent support in every situation. I am very thankful to my friend Mr. Sumesh K.C for his help and support during my experiment in the research.

Finally, my sincere acknowledgement to King Mongkut's Institute of Technology Ladkrabang for providing financial support and instruments to conduct this research and also Thailand Research Council for the grant of the integrated research budget in the fiscal year of 2017 for the research. I am very thankful to my teachers and friends who helped me directly and indirectly to conduct this research.

Sneha Sharma

Table of contents

Table of contents (continued)

Table of contents (continued)

List of Tables

List of figures

List of figures (continued)

Chapter 1

Introduction

1.1 Introduction to the research problem and its significance

Mango (*Mangifera Indica* L.) well known as the queen of fruit that has an excellent exotic flavor .Because of the wide distribution of the growing regions, these fruits are produced in 115 countries. Although Mango production is over in 100 countries, the large production is concentrated within 10 countries. According to the statistics, from January to December 2017, 30,783,364 kilogram of fresh mango worth 32,402,976 Baht were exported to several countries from Thailand [1] which represented a 29 fold increase and is listed on world's third largest mango exporting country for selected year since 2000 [2]. This data shows that, Mango production is playing a vital role in increasing the economic standard of Thailand .In order to increase the export rate of mango, the quality attributes of the fruit should be maintained accordingly .Thus, to maintain the quality of fruit advance technologies in the production plant should be developed.

The traditional quality control method are moreover based on the manual sampling and destructive measurement. The process involved in such method are slow and that arises the problem of quality degradation because of the time lag between product processing and actual result [3]. Therefore, conventional methods for the determination of quality parameters are very time consuming and labor intensive [4]. Also, the fruits are damaged after the destructive analysis for measuring different parameters which is not the feasible solution for the fruits like Mango. In order to check the quality of fruit after harvesting there is the need of quick and non-destructive method so that the fruit remain unharmed and the quality can be analyzed within few minutes before it is ready to export.

One of the possible way to solve the mentioned problem is the use of online detection techniques. There are several advantages of these techniques such as it can be assembled in the production line and can be used for real time condition, any sign of possible failure can be detected early, assessment of condition at any desired time is possible and permanent monitoring of the system can be done [5]. Fruits and vegetables of same kind may have different shape, size, color, taste and chemical compositions even when they are harvested at the same time .It is now

important for the farmers to know the difference among the same variety of fruits and sort them on the basis of their quality.

According to Sirisomboon (2013), NIR spectroscopy measures the interactions between the electromagnetic radiation in the NIR region (780-2500 nm) and the molecules in the analytes. NIR spectroscopy technique has shown its performance on evaluating different parameters in fruits and vegetables. NIR spectroscopic technique can provide rapid results in seconds or continuously online, rather than in hours or days, with an accuracy and reproducibility equivalent to most reference methods. As the main advantages of NIR include cost efficiency, no uses of harmful chemicals, flexibility in sample presentation and continuous testing. NIR spectroscopy is the method based on molecular overtone and combination vibration of C-H, O-H and N-H bonds. Total soluble solids contain sugar compound mainly sucrose which molecular structure consist of C-H and O-H band, so the NIR spectroscopic techniques can be used to analyse the TSS content in fruits.

Many research has shown the robustness of the model in laboratory condition (offline) but online monitoring condition for quality analysis is more desirable nowadays. Although there is requirement of the online monitoring techniques and several researches are ongoing, the acquisition of spectral data during an online process, on a conveyor belt or through a pipe, is quite complex [7]. Spectral acquisition from a moving sample depends on particle size, shape, orientation, type and also composition [8].

Sanchez 2012, reported that increasing awareness of the consumer on food quality has led to emphasize more on the fruit's sorting systems based on internal quality attributes. The commercial application of NIR spectroscopy in fruit grading lines at pack-houses, for sorting fruits by its SSC, was initiated in Japan in the mid 1990s. Use of the NIR sensors in the grading line are applicable for fruit sorting system. Since, the system still lack the accuracy so this issue has been subject of some reviews [10-13], although the research on target specific is limited.

Some researches done by using the concept of online monitoring has shown its feasibility. The use of NIR spectroscopy for determination of sugar content in intact peaches and mandarins, and reported an automated fruit sorting machine based on this principle by Kawano et al. [14, 15]. Similarly, Choi 1998, used NIR reflectance spectroscopy in order to develop an online machine based on the real time determination of sugar content. Result with a low SEP of 0.78 °Brix was obtained in Fuji apples with minimum error such errors were acceptable for rapid online detection. He et al. [17] detected sugar content, acidity and internal browning in oranges and apple using the online reflex, the partially shaded light transmission and fully shaded light transmission. The result obtained was satisfactory with R^2 of 0.95

for °Brix, and 0.85 for acidity. Miller and Zude 2002, [18] used both the online commercial NIR equipment and hand-held NIR units were used to measure °Brix level of Florida citrus. Salguero-Chaparro and Rodriguez, 2014 [19] performed online versus off-line analysis of intact olives and draw the conclusion that the combination of a portable diode-array spectrometer with an adequate regression method is feasible to meet the industrial requirement for an online, fast, simple and cost-efficient screening analysis different quality parameters in directly in the process line.

Therefore, we propose a research of feasibility study on online measurement of quality parameter of mango using NIR spectroscopy for real time environment .NIR spectroscopy has been used for at lab condition for determination of total soluble solids of mango .We would like to research if we can develop a model for real time condition that can be beneficial for the large mango production or distributor firm.

1.2 Objective

The overall objective of this study was to find the possibilities of using rapid evaluation method, NIR Spectroscopy to determine total soluble solids of mango in real time conditions .The specific objective were-:

[1] To study the NIR spectral characteristics of Mango using online and offline scanning condition.

[2] To study the feasibility on online monitoring of intact mango fruit using Near Infrared (NIR) Spectroscopy.

[3] To develop the partial least squares (PLS) regression model using shortwave Vis-NIR spectrometer and full wave NIR spectrometer for measuring total soluble solids in Mango.

1.3 Scope of Research

In this research, Namdokmai Sithong variety of Mango, which is very popular in Thailand, was used .For online scanning Vis-NIR range of 600-1000 nm was selected, similarly for offline NIR range of wavelength 800-2500 nm, wavenumber (12,500-4,000 cm^{-1}) was selected .Total soluble solids of mango was measured and model was developed using Partial Least Squares Regression (PLSR). The spectral characteristic of NIR scanning performed by both online and offline condition was studied.

1.4 Expected Result

This research was proposed in order to find the effective solution for the Mango production firm in order to determine the quality of exporting fruit. So, this research will be useful for quality monitoring of the Mango by non-destructive technique after harvesting in the farm. This research will determine the feasibility of using short wave Vis-NIR spectrometer for online scanning condition for measuring total soluble solids of Mango.

1.5 Experimental Design

The experiment was divided into two parts, online scanning and offline scanning. The Figure 1.1 shows the experimental plan for preliminary test. The experiment was performed to determine the precision of the NIR instrument and reference laboratory by calculating the maximum coefficient of determination (R^2_{Max}) which indicated whether the standard reference method can be used for measuring total soluble solids of Mango from repeatability and reproducibility test. After obtaining the precision of the instrument and reference laboratory further experiment was planned as shown in Figure 1.2.

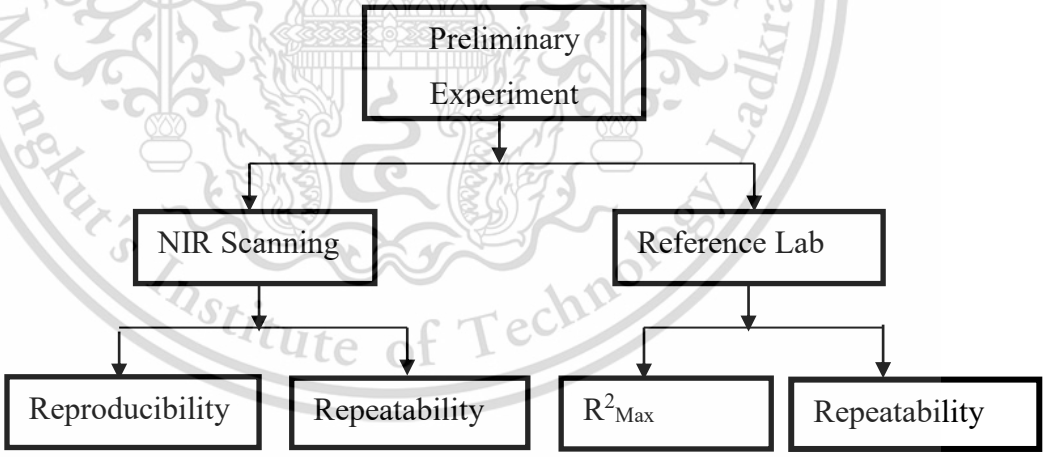

Figure 1.1 Preliminary experiment plan.

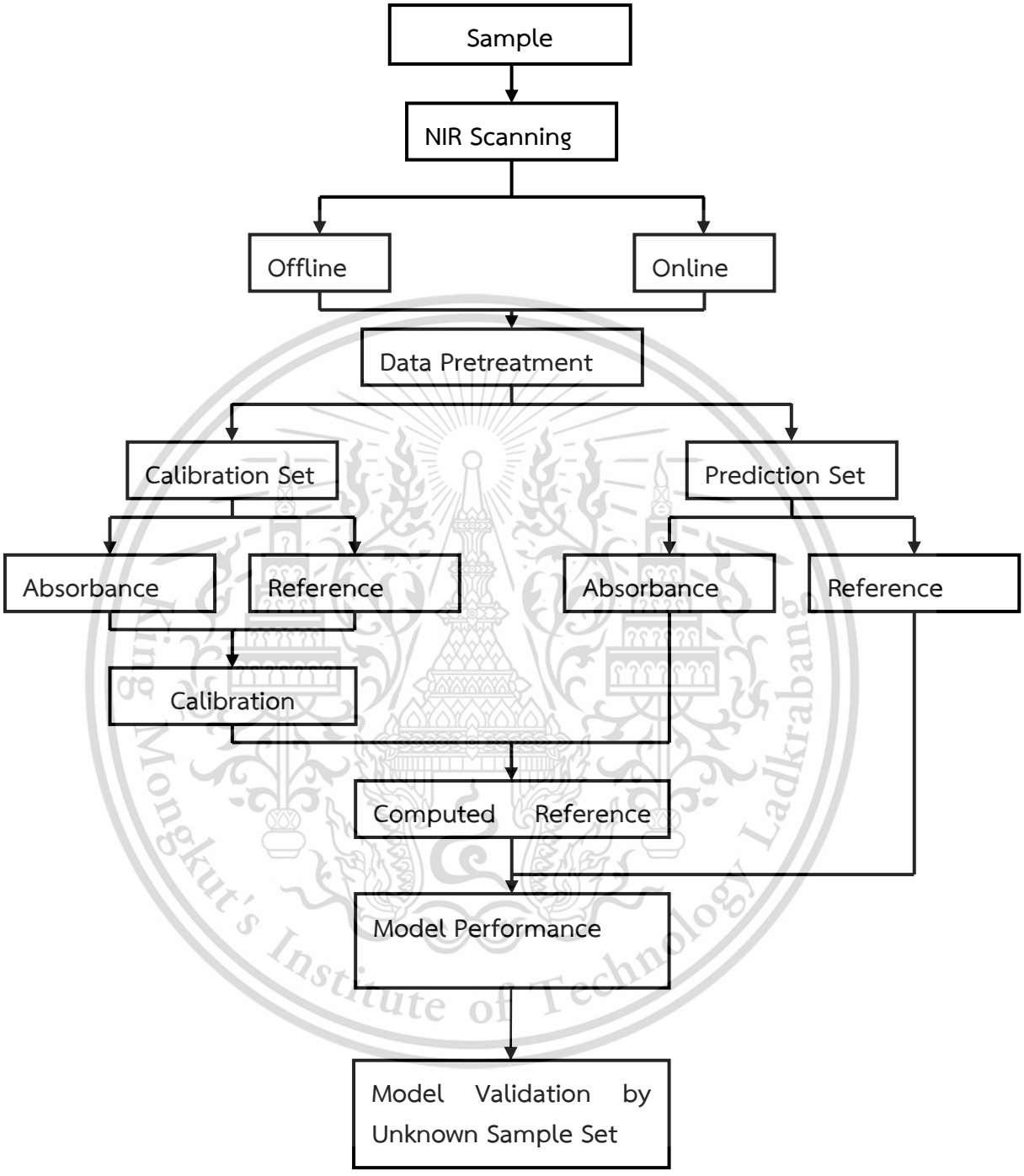

Figure 1.2 Experiment plan.

Chapter 2

Theory and Literature Review

2.1 Mango

Mango is one of the exotic tropical fruits and is widely produced in the world for its attractive color, good taste and high level of health-beneficial compounds. Mango is a fruit having high nutritional value, supplying the human diet with calories and nutrients such as fiber, vitamins, and minerals. It can be considered as a functional food, due to the presence of a large number of bioactive compounds that are beneficial in improving the health and reducing the risk of chronic degenerative diseases [20]. Mango fruits contains high amount of carotenoids and important vitamins such as Vitamin A, C and E [21]. Namdokmai Sithong is one of the popular variety of mango which was originated from Thailand. This variety has the appealing looks and good taste that leads to the increasing demand of fruits among the costumers all over the world. The shape of the fruit is oval with pointy tip. The unripe fruit is green and can be very sour and the fully ripe one has beautiful golden colored skin with creamy yellow shades and sweet in taste. Each mango can weigh up to 300-400 grams [22]. This variety is available throughout the year, though the peak available time is from January to July. Mango fruit of various cultivar differ greatly in shape, appearance and internal characteristics [23]. The characteristic taste and flavor of the mango cannot be attained unless the fruit is harvested at the appropriate stage of maturity. The postharvest quality of mango can be measured by the dry matter (DM), firmness, fruit color (both peel and flesh), total soluble solids (TSS), titratable acidity (TA) and aromatic compounds [24-27]. Although mango production is an important activity worldwide, problems related to fruit quality limit the consumption of this fruit. One of the main problems is marketing fruits with different maturity stages and consumer quality in the same batch [28]. Post-harvest handling of this fruit is very essential because of its firm and soft nature. Small impact on the skin during the harvesting stage can ruin the whole fruit. The analysis of the internal quality of Mango has been done by both destructive and nondestructive techniques [29, 30]. Though the rapid nondestructive quality analysis of fruit in the firm and production house is still in high demand.

2.2 Total Soluble Solids (TSS)

The TSS is a refractometric index that indicates the proportion (%) of dissolved solids in a solution. TSS is the sum of sugar, acids and other minor components in the fruits [31]. During the ripening stage of mango there is increase in the soluble sugar content which is usually expressed as TSS as most of the solids are sugar [32]. Total soluble solids content and to a small extent of sucrose, glucose and fructose are the typical quality attributes for assessing the sweetness of Mango and have shown the usefulness in determining the physiochemical changes during the ripening stages [33]. The sugars were identified as glucose, fructose and sucrose in four mango cultivars by Liu et al, [34], and among which sucrose was the predominant sugar in four mango cultivars. Total soluble solids concentration is represented in TSS% or °Brix. Jha et al, [35] during their research reported that, TSS in mango increases from 6.9-8.1 °Brix till reaching to the maturity stage and gradually increases from 8-13 °Brix after attaining the maturity. The TSS content of stored fruit increases up to 19 °Brix.

Bradley, 2010 [36] described different methods to measure TSS. TSS is measured using the digital and hand held pocket refractometer. The refractometer has been valuable in determining the soluble solids in fruits and fruit products (AOAC Method 932.12; 976.20; 983.17). When the light beam passes a specific wavelength through a glass prism into a liquid in the refractometers, it provides the reading. Different types of refractometers are available, some refractometers are designed only to provide results as refractive indices, and some hand-held refractometers are equipped with scales calibrated to read the percentage of solids, percentage of sugars. Summary of the different type of refractometers used in the post-harvest research of different type of fruits like apple [37], orange [38], pear [39] and many more are reported by Magwaza and Opera, 2015 [40]. TSS of fruits and vegetables can also be measured by using gravimetric methods using hydrometer [41].

2.3 Near Infrared (NIR) Spectroscopy

In the 19th century, Sir William Herschel discovered the presence of energy beyond the visible red spectrum during his experiment and further named the region “Infrared”. Infrared region of electromagnetic radiation is divided into three regions, Near Infrared, Mid Infrared and Far Infrared respectively. Among these regions Near Infrared region range from 700 nm to 2500 nm. NIR spectroscopy is a spectroscopic technique that uses the NIR region of electromagnetic radiation. The NIR

spectroscopic instrumentation and its development were concerned, credit has been given to the researchers in agriculture science, foremost Karl Norris, who has recognized the potential of this technique from the very early stages of its development [42]. The gradual increase in the development of NIRS instrumentation has been observed since last few decades.

NIR spectroscopic technique is based on the measurement of NIR radiation absorbed, reflected or transmitted by the component of the sample that has to be determined. Each radiation has interaction with the molecules in the different way. Sandorfy et al. [43] explained the fundamental vibrations of molecules lead to absorption in the infrared (200–4000 cm^{-1}), while their overtones and combination tones appear in the infrared and in the near infrared. The NIR spectrum is located between the infrared and the visible, from 2500 nm to 800 nm or from 4000cm^{-1} to 12,500cm^{-1}. It is sometimes called the overtone region. Certain groups of atoms, such as carbon-hydrogen C-H, oxygen hydrogen O-H, and nitrogen-hydrogen N-H are known as functional group that is present in most of the agricultural products. Absorption at different wavelength from (700-2500 nm) during the interaction of the NIR radiation can be assigned to these functional groups [44].

2.3.1 Basic Principle of NIRS

Osborne et al. [45] considered electromagnetic radiation as simple harmonic wave to explain the properties, but the phenomenon related to the absorption or emission of energy during the interaction with the molecule is not considered in the wave model. In order to explain the phenomenon based on the absorption, Siesler, 2007 [46] considered the harmonic diatomic oscillator model, where the vibrating masses m_1 and m_2 led to change in the internuclear distance. This model gives the molecular frequency of the diatomic oscillator (ν)

$$\nu = \frac{1}{2\pi}\sqrt{\frac{k}{m}} \qquad (2.1)$$

where, k is the force constant and the reduced mass *m* is given by (m_1 m_2)/(m_1+m_2)

According to the quantum mechanics, molecules can only exist in quantized energy states. Thus, vibrational energy is not continuously variable but rather can only have certain discrete values. Under certain conditions a molecule can transit from one energy state to another $\Delta\nu = \pm 1$, in case of harmonic oscillator is given by equation (2.2) [47].

$$E = (\nu_i + 0.5)\, h\nu,\ \nu_i = 0, 1, 2 \qquad (2.2)$$

As a conclusion to the harmonic model by Miller 2001 [48], it was noted that when all molecular vibration are assumed to be harmonic, all molecular transition starts at the lowest possible vibrational energy v=0 to 1, only fundamental transitions are allowed and this would eliminate the probability for the absorption in the NIR range as discussed above. Most real molecules undergo anharmonic, rather than harmonic vibrations.

Anharmonic model for diatomic model explained by Osborne et al, [45], as two atoms approach one another coulombic repulsion between the two nuclei cause the potential energy to rise more rapidly than harmonic approximation prediction. As the interatomic distance approach at which dissociation occurs, the potential energy level is off. In that case the an empirical function due to Morse, which fits the solid curve in to a good approximation is,

$$E = E_D\,(1 - e^{-\alpha y})^2 \qquad (2.3)$$

where, α is a constant for a particular molecule and E_D is the dissociation energy.

Solving equation 2.3 using the wave mechanical equations for anharmonic oscillator,

$$\Delta E = h\nu\,[1-(2v+\Delta v+1] \qquad (2.4)$$

and Δv = ±1, ±2, ±3. Thus anharmonicity model can explain the interaction of the NIR radiation on the molecules with the presence of fundamental, overtone and combinational vibrations.

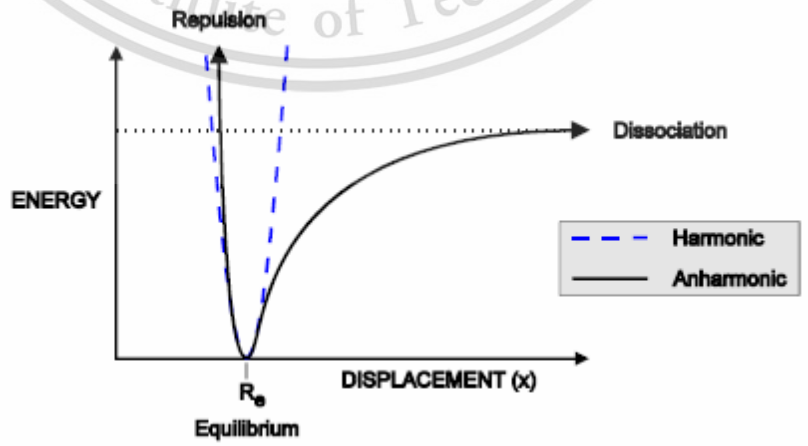

Figure 2.1 Harmonic and anharmonic oscillation [49].

2.3.2 Offline NIR Spectroscopy

Offline analysis is also useful for the control of a process or manufacturing operations. In this type of analysis, manual sampling is required. Samples are measured intermittently, as for offline measurements, but in this case, the spectrometer is located in a space very close to the industrial process itself [50]. Laboratory analysis are commonly done using the offline NIR spectrometers. Basically, large number of research based on spectroscopic techniques are done in laboratory conditions. Sample preparation and the operation procedure is easier using offline analysis technique rather than the online/in-line technique.

2.3.2.1 Fourier-Transform (FT) NIR spectrometer

One of the instrument that can be used for offline NIR spectroscopy is FT-NIR spectrometer. FT-NIR spectrometer measure the concentration of the analytes in absorbance, transmittance and diffuse reflectance mode. The FT-NIR spectrophotometer displays many of the common sampling options used in the NIR [51] Integrating spheres or other types of diffuse reflectance accessories are utilized heavily in the NIR. FT-NIR technology offers a lot of advantages it is quick, cost-effective and safe, since no hazardous chemicals are used. It simply measures the absorption of near-infrared light of the sample at different wavelengths [52].

2.3.2.2 Michelson Interferometer

This method use dispersive technique discovered by Michelson for measuring the spectra so the technique is known as the Michelson Interferometer. This technique consists of a fixed mirror, one movable mirror and beam splitter. When the incident ray of light passes toward the beam splitter the radiation is divided into two rays. One ray travels to the movable mirror and another ray passes through the fixed mirror and reflected back to the beam splitter. Then the output beam from the beam splitter is detected by the detector placed. As mirror B moves, a phase difference is introduced between the two beams, and constructive and destructive interference occurs optical path difference changes through multiples of the wavelength [53].

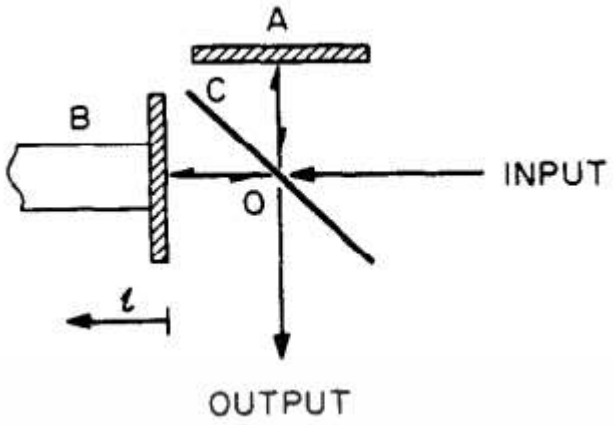

Figure 2.2 Schematic diagram of a Michelson interferometer showing the fixed mirror (A). the moving mirror (B), and the beam splitter (0 The center of the beam splitter is denoted by (0). and the optical path of a parallel light ray is denotedby the arrows [53].

2.3.3 Online NIR Spectroscopy

Online NIR analysis is performed by measuring the spectra on a continuous flow of sample passing through a flow cell. In such experimental setup the sample is analyzed while the process is operating [54]. Nowadays the availability of fiber optics probe and the speed of NIR make them suitable for remote and online sensing of particle size also providing the chemical information [55]. Diode array spectrometer are considered to be the best alternative for fast scanning in online or inline analysis [56].

2.3.3.1 Diode Array Spectrometer

Choi (n.d.) [57] describes the basic principle of diode array spectrometer, as the polychromatic beam from the source is irradiated onto the inlet slit of the after passing through the sample compartment, the radiation is dispersed by the dispersive device such as prism or holographic grating into the narrow band of the spectrum onto the diode array. The photodiode converts light into electrical signals and temporarily stores them.

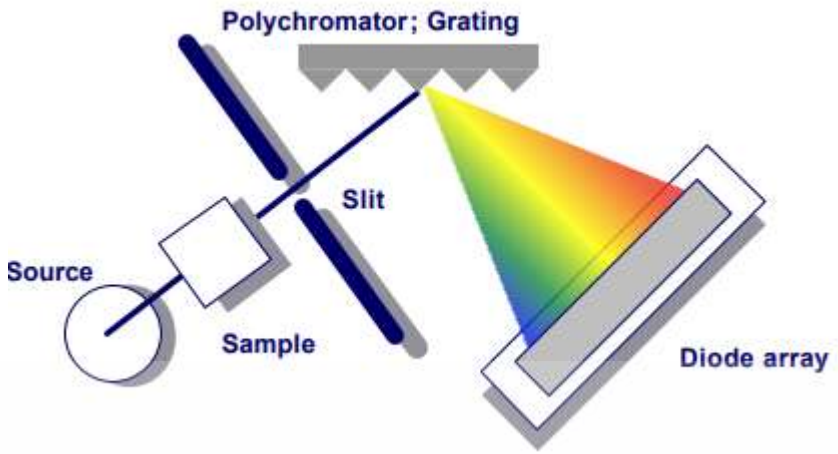

Figure 2.3 Diode array spectrometer (Choi, n.d.) [62]

2.3.4 Sample Presentation

NIR spectroscopy has basically four types of sample presentation: Transmittance, Reflectance, Transflection and Interactance. These sample presentation options normally involve the use of separate, detachable accessories and include the option of using fiber-optic probes for spectral acquisition from remote sites within a large industrial complex, for example, petrol refineries and pharmaceutical production facilities [58]. The widely used sample presentation in modern NIR spectrometers is reflection mode among all the other options.

2.3.4.1 Absorption and Transmission

When the electromagnetic NIR radiation falls into the samples many modes of interaction occurs. But, mostly, we are concerned with the phenomenon of absorption of radiation. If the sample is simply illuminated with one wavelength of radiation after another, one at a time, and the variation of transmission with wavelength is measured, the spectrum is obtained [59]. The absorption intensity is a function of three factors as explained in detail by Osborne, et al, [45], according to the Beer-Lamberts law, the transmittance is converted to the absorbance,

$$A = \log (1/T) \tag{2.5}$$

and the absorbance is given by,

$$A = abc \tag{2.6}$$

where, A is absorbance, a is the absorptivity ($mol^{-1}lcm^{-1}$), b is the thickness through which radiation passes and c is the concentration of sample. Therefore, we

can relate the concentration of sample with both absorbance and transmittance for the interpretation of spectra.

2.3.4.2 Reflection

If the sample is homogeneous and non-scattering liquid the Beer's law is satisfied, but if the sample is powdery or granular material, non-homogeneous and scattering Beer's law is not completely satisfied [55]. When the radiation passes through the weakly absorbing material it is reflected in both specular and diffuse reflection. Only diffuse reflection provides information on the nature of the surface. The theory of diffuse reflection is very complex and is still incomplete. The most widely accepted model was developed by Kubelka & Munk [60]) and relates the diffuse reflectance, *R,,* of an infinitely thick sample to the molar absorption coefficient, *k,* and the scattering coefficient, *s* [61].

$$\frac{(1-R_\infty)^2}{2R_\infty} = \frac{k}{s} \tag{2.7}$$

As explained by Osborne et al, [45], the absorbance coefficient *k* in the equation is equal to the multiplication of concentration (c) and absorptivity according to Beer-Lambert law.

$$\frac{(1-\mathrm{R}_\infty)^2}{2\mathrm{R}_\infty} = \frac{\mathrm{a}*\mathrm{c}}{\mathrm{s}} \tag{2.8}$$

For a practical purposes the diffuse reflectance is measured with respect to a non-absorbing standard and converted to the common logarithmic to produce nearly linear relationship with the concentration.

$$\log\frac{\mathrm{R}'}{\mathrm{R}} = \log\frac{1}{\mathrm{R}} + \log\mathrm{R}' = \frac{\mathrm{ac}}{\mathrm{s}} \tag{2.9}$$

R'= Reflectance of the standard and R of the sample $(R' > R)$. For monochromatic light R' is constant and can be ignored. Therefore

$$\log\frac{1}{\mathrm{R}} = \frac{\mathrm{ac}}{\mathrm{s}} \tag{2.10}$$

The presence of scattering causes increase in the path length hence apparent increase in A. The equation represents the mathematical model in which the NIR spectroscopic analysis is depend upon.

2.3.5 NIR Instrumentation

2.3.5.1 Light Source

Tungsten halogen light bulb is the most commonly used visible, ultraviolet, near infrared light source with (wavelength ~2.5 μm). The main characteristic of halogen light source is it consists of small quantity of active halogen gas filled in the lamp. This type of light source is inexpensive, with higher stability and longer life [62]. Light Emitting Diodes (LED) is another light source used for narrow waveband ranging from 600-900nm. The intensity of this source is higher than the tungsten halogen light bulb. LEDs surpass incandescent lamps through their longer lifetime, high brightness, low power consumption and the possibility for electrical modulation. The disadvantages of LEDs often faced in demanding sensor applications are a high sensitivity of wavelength and intensity to variations in operating temperature as well as a gradual degradation of optical output in the course of operating time [65].

2.3.5.2 Fixed and Variable Filters

Filters are the first method to be used in spectrometry for wavelength selection. Filters are fixed or variable such as interference filters, multiple filter Light Emitting Diodes (LEDs), Acousto-optical tunable filter (AOTF), Liquid crystal tunable filter (LCTF) are the type used in NIR spectrometers. Interference filters have a bandwidth of 10±2 nm and a peak transmission of 40% and are usually mounted in a rotating wheel [66].

2.3.5.3 Diffraction Grating

Diffraction grating is the type of instrument commonly used to split the beam of radiation in spectrometers. It is a collection of reflected or transmitted elements separated by a distance comparable to the wavelength of radiation. An electromagnetic wave incident on a grating will, upon diffraction, have its electric field amplitude, or phase, or both, modified in a predictable manner [65]. Diffraction grating consist of plate or a metal mirror engraved with a large number of parallel lines or grooves, which produces a spectrum when light passes through or is reflected [66].

2.3.5.4 Prism

There are three types of prism, dispersion, reflection and polarization. Dispersion and reflection type prism are widely used for spectrometers [67]. In spectrometers, prism is used to split the incident light into spectrum of different

wavelength. The dispersion of the prism depends upon the refractive index of the prism material and wavelength. Prism can provide wide range of spectrum although the dispersion is low as the wavelength increases. [68].

2.4 NIR Spectroscopy Model Development

Multivariate calibration is a method for finding the relationship between one set of measurement which is easy or cheap to acquire such as NIR data in spectroscopic techniques and other data which are either expensive or labor intensive [69]). Cluster of data set is obtained from the NIR instrument for prediction of constituents in the analytes. These data are analysed using multivariate analysis which is very important part in chemometrics. Chemometrics is the branch of science which deals with mathematical and statistical methods to solve understand the chemical information and correlate the quality parameters or physical properties to analytical instrument data [70]. NIR instrument measure the constituent by log (1/R) values that must then be related to the amount of the component determined by some other methods called Reference or Standard methods [71]. This relationship is established using the multivariate analysis such as Principal Component Analysis (PCA), Partial Least Squares Regression (PLSR). Before calibration modeling the spectra is treated by some preprocessing techniques in order to remove the unwanted factors such as noise, baseline shift, scattering effects.

2.4.1 Data Pretreatment

2.4.1.1 Smoothing

Smoothing is a method to reduce the noise in the spectrum. There are two types of smoothing: running mean smoothing and Savitzky-Goley. Running mean simply replaces the value at each point by the mean of the values in the wavelength surrounding it. The advantage of this type of smoothing is ease to calculate. On the other hand, Savitzky-Goley is based on principle to fit the spectrum in a wavelength interval with a polynomial by least square method, and the parameters are the degree of the polynomial and number of point to fit [71].

2.4.1.2 Derivatives

Derivative are applied to the spectral data in order to enhance the appearance and improve calibration for the constituents [71]). It simply calculates first and second derivative of the spectrum. First derivative, the signals with steep edges will get more emphasis than the signal with relatively flat bands. But with the

second derivative even more flat bands can be evaluated [72]. The main drawback of this derivative pretreatment is the enhancement of spectral noise after using this preprocessing.

$$X'_I = X_i - X_{i-1} \quad (2.11)$$

$$X''_I = X'_i - X'_{i-1} \quad (2.12)$$

Where, X'_I denotes the first derivative and X''_I the second derivative at point wavelength (i) [73]

2.4.1.3. Normalization

This method suppresses the unwanted sources of variability by making a group of spectra having more common features. There are different type of Normalization such as Mean Normalization, Max Normalization and Range Normalization. Normalization is used to eliminate the influence of different optical path lengths in case of transmission measurement. Similarly for diffuse reflectance the interfering influence of different material densities or particle sizes can be minimized by Normalization (Conzen, 2006 [72].

Mean Normalization

In Mean Normalization each row in data matrix ($X_{i,k}$) is divided by its average value $\overline{X}$ [74].

$$X_{i,k} = \frac{X_{i,k}}{|\overline{X}|} \quad (2.13)$$

Maximum Normalization

In this normalization each row in data matrix ($X_{i,k}$) is divided by its maximum absolute value $Max|X_i|$ [74].

$$X_{i,k} = \frac{X_{i.k}}{Max|X_i|} \quad (2.14)$$

Range Normalization

In this normalization each row in data matrix is divided by the range of the total value (max value –min value) [74]).

$$X_{i,k} = \frac{X_{i.k}}{Max(X_i) - Min(X_i)} \quad (2.15)$$

2.4.1.4 Multiple Scatter Correction (MSC)

In order to remove the scattering effect and baseline correction in the spectra The technique to calculate MSC explained by Buddenbaum and Steffens (2012) [75], in this preprocessing the mean spectrum X(i) is considered the ideal spectrum. This spectrum represent mean scattering and offset. Each spectrum X(i)' is then fit to the mean spectrum using the least square method

$$X(i)' = u + v\,X(i) \tag{2.16}$$

where, $X(i)'$ is the transformed spectra, $X(i)$ is the mean spectra and u and v are chosen such that the difference between the mean and transformed spectra is minimum. Hence, the MSC spectrum is calculated by determining the coefficients for each spectrum and then transforming the spectrum as,

$$MSC_i = \frac{X(i)' - u}{v} \tag{2.17}$$

2.4.1.5 Standard Normal Variate (SNV)

SNV is a transformation usually applied to spectroscopic data in order to center and scale each individual spectrum. SNV is sometime used with Detrending in order to reduce multicollinearity, baseline shifting and curvature in the spectrum. [76])

$$SNV = \frac{X - \bar{X}}{SD(X)} \tag{2.18}$$

where, X is the individual value in a row $\bar{X}$ is the mean value of the row.

2.4.2 Calibration Method

Sanchez, 1991 [77] explain the multivariate calibration and validation in detail. The calibration method is used to establish the calibration equation or model for prediction between the measured values by NIRS usually absorbance (X) and the concentration of analyte measured by standard method (Y). There are two different objectives to establish the calibration equation, for predicting the constituents in the sample (quantitative analysis) and for classifying group of samples (qualitative analysis). Multivariate regression modeling like Multiple Linear Regression (MLR), Partial Least Squares Regression (PLSR), Principal Component Regression (PCR), is used for quantitative analysis. Principal Component Analysis (PCA), Partial Least Squares Discriminant Analysis (PLS-DA) is used for qualitative analysis.

MLR is used to quantify the relation between a set of independent variable (X) and a single dependent variable (Y). But, MLR is not usually preferred for multivariate calibration because the number of available sample is much smaller than the number of x-variable and this leads to the problem of multicollinearity [78]. PCR is full spectrum method for the quantitative analysis as it uses all the information of the full spectrum and compresses it into a number of small variable. It reduces the amount of optical data (x-data) by constructing small amount of factors known as Principal Components (PC). PCR in a way solve the problem of multicollinearity, but it can only explain the variance in X variable by converting it into the score and loading and does not used the information related to the Y variables. PLSR is the method that uses both the information between data matrix (X) and concentration matrix (Y) [78].

2.4.3. Partial Least Squares Regression (PLSR)

PLSR is widely used multivariate technique that uses both information related to X and Y variable in the data set. PLS regression solves the problem of PCR by relating the spectral data and property of interest with the outer relation called latent variables or loading weights and also endures the maximum correlation between them during calibration and compresses the data in such a way that most of the variance in both X and Y is explained [79-81]

The algorithm for PLS NIPALS is given below explained by Shrestha, 2016 [82] with the graphical representation by Andrade-Garda et al. [79].

In X-block

Let u_1= any y (reference value)

Calculating the weight of X-block using the score of Y-block

$$w_1^T = \frac{u_1^T X}{u_1^T u_1} \tag{2.19}$$

$$w_1^T = \frac{w_1^T}{\|w_1\|} \text{ (normalizing)} \tag{2.20}$$

defining the X-score using original X-data

$$t_1 = X w_1 \tag{2.21}$$

in Y-block

using X-score to calculate the Y-loading

$$q_1^T = \frac{t_1^T Y}{t_1^T t_1} \tag{2.22}$$

Calculating Y score,

$$u_{1,new} = \frac{Y\, q_1}{q_1^T q_1} \tag{2.23}$$

the inner relation is given as

$$\widehat{u_1} = b_1 t_1 \tag{2.24}$$

The inner regression coefficient is

$$b = \frac{u_1^T t_1}{t_1^T t_1} \tag{2.25}$$

calculating X-block loading

$$p_1^T = \frac{t_1^T X}{t_1^T t_1} \tag{2.26}$$

Calculation of residual

$$E = X - t_1^T p_1 \tag{2.27}$$

$$F = Y - b t_1^T q_1 \tag{2.28}$$

Finally regression coefficient vector is

$$b = W(P^T W)^{-1} q \tag{2.29}$$

$$q = (T^T T)^{-1} T^T y \tag{2.30}$$

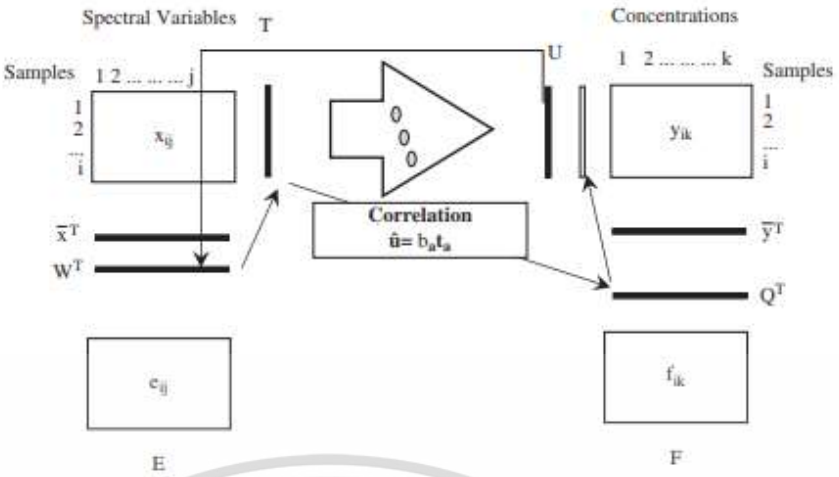

Figure 2.4 Calculation of regression coefficient between t and u of PLS model [79].

2.5 Model Performance

2.5.1 Coefficient of correlation (r)

Correlation coefficient (r) shows the degree to which two X from NIRS and Y from the reference lab agree with each other. If X and Y correlated with each other completely r-value will set 1.000 but in the real situation X and Y data exhibit some error which is unavoidable which will not allow the correlation to be 1.000. The X and Y data may be correlated either positively or negatively [44].

$$r = \frac{\sum(X*Y)-[(\sum X*\sum Y)/N]}{\langle\{\sum X^2-\left(\frac{\sum X^2}{N}\right)\}*\{\sum Y^2-\left(\frac{\sum Y^2}{N}\right)\}\rangle^{1/2}} \quad (2.31)$$

2.5.2 Coefficient of determination (R^2)

The coefficient of determination (R^2) shows the proportion of the variance in X data that can be explained by the variance in the Y data. For example if R^2 is given 0.950 that means 94.1% of the variance in X can be explained by the variance in Y. and 5 % of the variance in X is attributable to other factors such as sample preparation, reference testing and so on. R^2 is given by the formula [83].

$$R^2 = 1 - \frac{\sum(X-Y)^2}{\sum(X-\overline{X})} \quad (2.32)$$

X is the reference value, Y is the predicted value, $\overline{X}$ is the mean of X (Conzen, 2006) [72].

2.5.3 Standard error of Prediction (SEP)

SEP is the SD of differences between NIR reflectance and reference value. SEP should be computed from the results of the prediction of set of samples that have not been used in the development of the calibration. The sample set is prediction or validation sample set [83].

$$\mathrm{SEP} = \sqrt{\frac{\sum(\mathrm{X}-\mathrm{Y})^2 - \frac{\sum(\mathrm{X}-\mathrm{Y})^2}{\mathrm{N}}}{(\mathrm{N}-1)}} \tag{2.33}$$

2.5.4 Ratio to SEP to SD (RPD)

Residual Prediction Deviation (RPD) value is the percentage of the standard deviation (SD) of the reference values and the bias-corrected mean error of prediction of the validation (SEP_{bias}) [44].

$$\mathrm{RPD} = \frac{\mathrm{SD}}{\mathrm{SEP_{bias}}} \tag{2.34}$$

2.5.5 Bias

Bias is the systematic averaged deviation between the data set of the true and the predicted value. It is calculated by averaging all the particular deviations between the data sets [72].

$$\mathrm{Bias} = \frac{\sum_{i=1}^{M} Y_i^{meas} - Y_i^{pred}}{M} \tag{2.35}$$

2.5.6. Root Mean Square Error of Estimation

Root Mean Square Error of Estimation calculates the analysis error of the calibration set [72]. RMSEE can be calculated using the equation (2.36) where, M is the number of sample and R is the rank or factor used.

$$\mathrm{RMSEE} = \frac{\mathrm{SSE}}{\mathrm{M}-\mathrm{R}-1} \tag{2.36}$$

2.6 Validation Method

After obtaining a calibration model or equation, the model is used to determine the percentage of constituents in a set of special samples also called “unknown”. Comparison of NIR instruments and reference method measurement on a new set of samples provides a basis for calculation of the true measurement error.

This comparison is called validation of the calibration model [71]. This validation can be done by two methods full cross validation and test set validation.

2.6.1 Cross Validation

Cross validation is the validation techniques based on calibration data set. In this technique, first, sample one in the calibration set is deleted. Then the calibration is performed on the rest of the sample before it is tested on the first sample by comparing $\widehat{Y}_i$ and Y_i. Then the first sample is placed back and the process is repeated by deleting sample two [78]. The differences between the predicted data and reference data, which is also called the residual is the root mean standard error of cross validation.

$$\mathrm{RMSECV}=\sqrt{\sum_{i=1}^{N}\frac{(\widehat{Y}_i-Y_i)^2}{N}} \tag{2.37}$$

2.6.2 Test Set Validation

Test set Validation is also known as external validation. In this validation the calibration model is set by using all calibration spectra and to validate the model, separate data set (unknown) with known concentrations are used. For large population this type of validation is used. Root mean square error of prediction (RMSEP) represents the quantitative measure for the predictive accuracy of test set validation [72]).

$$\mathrm{RMSEP}=\sqrt{\sum_{i=1}^{N}\frac{(\widehat{Y}_i-Y_i)^2}{N}} \tag{2.38}$$

2.7 Literature Review

NIR region of the electromagnetic spectrum as the wavelength range of 700–2500 nm corresponding to the wave number range 12820–3959 cm−1. NIR spectroscopy is a spectroscopic technique that uses NIR region of electromagnetic spectrum. The most prominent absorption bands occurring in the NIR region are related to overtones and combinations of fundamental vibrations of –CH, –NH, –OH (and –SH) functional groups [84]. Near Infrared Spectroscopy (NIRS) is known as a rapid technique to evaluate the quality traits of fruits and vegetables. Many researches related to the methods for implementation of NIRS has been successfully published and some are ongoing. There are several advantage of NIRS compared to some traditional chemical methods like fast speed, accuracy, minimal sample preparation, no use of toxic reagents, fast processing and result etc. Despite of these

advantages, limited work has been able to publish in the field of online monitoring by NIRS in industrial plant [85]. Some of the disadvantages of traditional NIRS laboratories instrument like low scanning speed, high cost and non-portable might be the reason of this limited implementation [8].

After several research and development of new technologies in the field of NIRS, in/online analysis has been proved to be one of the most efficient technique for controlling process and product quality in food processing industries [4]. Online detection techniques have advantages like it can be assembled in the production line in the real time condition, early detection of possible failures, permanent monitoring of the condition and assessment of conditions at any desired time [5]. By the use of diode array spectrometers online implementation of several parameters in fruits and vegetable is possible. From the research we came to know that NIR reflectance measurements allow obtaining valuable information about chemical and physical properties of several components in motion

Analytical techniques such as liquid chromatography using different separation techniques (reversephase, ion-exclusion, ion chromatography) and detectors (refractive index, UV absorption, amperometric), thin-layer chromatography, and gas chromatography have been commonly used for qualitative and quantitative analyses of fruit juices in order to detect several essential components [86]. NIRS has shown its high potential in measurement of several constituents in the intact fruits, vegetables and also for the food product during offline or at-lab conditions. As the molecular structure of sucrose consist of C-H and O-H overtone and combination bond, NIRS has shown feasibility in measuring sugar compounds in different fruits. Research has been done in many fruits including Apple [87], Peach [88], Pears [89] etc. for measuring the total soluble solids content using NIR spectroscopy in offline condition. Though the requirement of in-site or online measurement for quality analysis of different agricultural products has been increasing, only few research has been conducted for searching the possibilities of this technology for online conditions. Firmness and soluble solids (SSC) of the Red Fuji apples were examined by the Vis-NIR transmittance using the wavelength range from 650-920nm by Fan et al. [95] in order to determine the important factors to be considered for online measurement. In the research it was concluded that the NIR calibration equations developed by transmission spectra were sufficiently accurate to determine the internal quality, SSC and firmness, of apple nondestructively and it is possible to use this non-destructive technique for online detection of apple internal quality. NIR spectroscopic method with fiber optics in interactance mode was evaluated by Kawano et al. [14] for measuring SSC in the intact peach and obtained good prediction model with minimal error. He et al. [17] compared three NIR measuring

methods: the online reflex, the partially shaded light transmission and the fully shaded light transmission. They detected sugar content, acidity, and internal browning in oranges and apples by a fully shaded light transmission detecting device. Satisfactory results were obtained with $R^2$of 0.95 for °Brix, and 0.85 for acidity. Several researches has shown the online measurement of the fruits using NIRS transmittance mode. For measuring the quality of products at the real time situation Choi (1998) [16] has built up an apple sorter using the photodiode reflectance NIR spectrometer and similarly a feasibility study was conducted to measure grain quality (moisture and protein content) with near–infrared reflection (NIR) technology combined with harvestor by Maertens et al. [9]. There is a possibility of using NIRS for online quality analysis in fruits specially the total soluble solids content which is one of the key factor for determining the quality of mango.

CHAPTER 3

Methodology

3.1 Preliminary Test

The test was conducted to obtain the precision of the NIR spectroscopic instruments that were used for the scanning of Mango and to test the precision of the reference laboratory method for measuring the TSS of mango. Repeatability and reproducibility of the online and offline instrument were calculated. In order to measure the precision of the reference laboratory, the repeatability test was performed and the maximum coefficient of determination (R^2_{max}) was calculated.

3.1.1 Sample Preparation

Sample, Mango cv. Namdokmai Sithong were brought from Chacheangsao province on June 3, 2017. The 3 mangoes were selected for the precison test in NIRS Research Centre of Agriculture Product and Food (www.nirsresearch.com), Department of Agricultural Engineering, Faculty of Engineering, King Mongkut's Institute of Technology Ladkrabang, Thailand.

3.1.2 Offline Scanning

The samples were scanned by using NIR Multi-Purpose Analyzer (MPA) Spectrometer (Bruker optics, Germany) with the scanning resolution of 16 cm^{-1} in absorbance mode and there were 32 scans for 1 average spectrum of the sample. Wavenumber was from 12,500-4,000 cm^{-1}. Gold plate was scanned as the reference background scanning before starting the sample scanning.

3.1.3 Online Scanning

For the online scanning, UV-Vis-NIR Spectrometer, AvaSpec-2048 - USB2 standard fiber optic spectrometer, wavelength range from 200-1160 nm was used. Integration time was set to be 3.7 ms using auto integration and a focal length of 2.5 mm approximately was set, according to the fruit size. White Teflon material was scanned for reference scanning. The sample was placed in a conveyor belt inside a black box.

3.1.4 Repeatability and reproducibility of the scanning test

Repeatability test was conducted by loading and scanning sample 10 times in the same position for both offline and online condition. And for the reproducibility samples were reloaded and rescanned for 9 times. After scanning by both conditions, three important wavelength were selected for calculating repeatability and reproducibility. The standard deviation of the absorbance log (1/R) obtained at the corresponding wavelength gave the repeatability and reproducibility.

3.1.5 Reference method

The samples were brought for reference laboratory after scanning. Each samples were cut into halves and total soluble solids of the samples were measured using Digital Hand-held "Pocket" Refractometer (PAL-1 S/No L218454, Atago Japan) and the distilled water was used as a calibration liquid.

3.1.6 Repeatability for reference method

Repeatability (Rep) of reference method can be defined as the standard deviation of the difference between the repeat measurements. Mango is divided into three parts to measure total soluble solids and each part has three repeat measurements. R^2_{max} was calculated then by using the formula

$$R^2_{max} = \frac{SD^2 - Rep^2}{SD^2} \tag{3.1}$$

where, SD was the standard deviation of repeat measurement of reference test.

3.2 Sample

Samples were brought from the mango orchard located in the Chacheangsao province of Thailand. Mangoes ready to be exported from the orchard were brought for the experiment. 200 samples were used for the calibration and 119 samples were used for the validation using the unknown sample set. Samples were placed in the room temperature of 25±1°C for 2 hours before scanning as shown in Figure 3.1. The fruit size was approximately 10 cm in length, 8 cm in width and 6.5 cm in height or thickness.

Figure 3.1 Sample presentation before experiment.

3.3 Online and Offline Spectroscopic Test

3.3.1 Offline NIR scanning

NIR scanning was done by using Fourier Transform (FT) NIR Multi-Purpose Analyzer (MPA) Spectrometer (Bruker optics, Ettlingen, Germany) range from 12,500-3,600 cm^{-1} (800-2,500 nm).

Samples were placed on the cylindrical aluminum platform of thickness 10 mm which was placed above the integrating sphere window as shown in Figure 3.2. Before scanning the sample, the gold plate was scanned as a background. Each sample was scanned on both side (A and B) with the scanning resolution of 32 cm^{-1} in absorbance mode. There were 64 scans for obtaining one average spectrum of the sample. For one Mango sample, two spectra were obtained, resulting a total of 200 spectra for developing a calibration model.

Figure 3.2 Scanning mango offline using FT-NIR spectrometer.

3.3.2. Online Vis-NIR scanning

Online scanning was done by UV-Vis-NIR AvaSpec-2048 - USB2 standard fiber optic spectrometer (Avantes, the Netherlands), wavelength from 200-1160 nm with integration time of 3.7 ms using auto integration and an approximate focal length of 2.5 mm. Before sample scanning calibration was done using a white reference Teflon material. For online scanning, 5 samples were placed at a time in a horizontal belt conveyor. Metal rods was attached in the conveyor to guide the sample. The speed of the belt was fixed at 0.11 ms^{-1}. Each sample was passed through the black box (60 cm long) which was attached on the conveyor, thus eliminating the influence of interference from the external light. Integrating sphere (Avasphere 50-REFL, Avantes, The Netherland) probe was placed in the middle of black box, mounting on the top of the black box as shown in Figure 3.3. The proximity sensor Arduino model E18-D80NK was fixed on the side of black box such that the probe and the proximity sensor were aligned in the same vertical plane. Since the samples were scanned during the motion, the proximity sensor acted as the external trigger for spectrometer. First, side A was scanned and then samples were reloaded in the conveyor for scanning side B simultaneously. In this way, two individual average spectra were obtained from one sample.

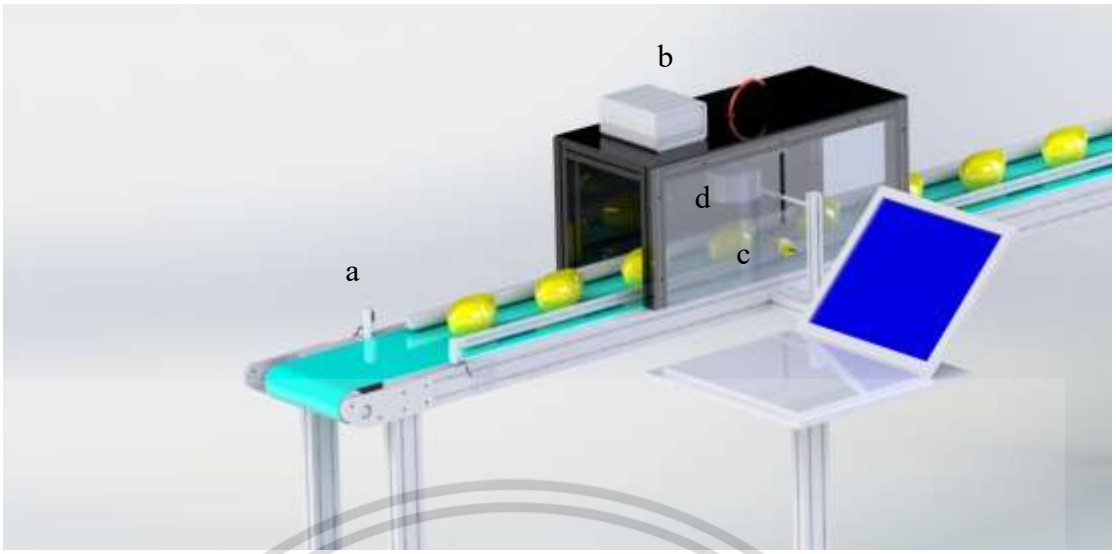

Figure 3.3 Online scanning system for measuring TSS of mango using UV-Vis-NIR Spectrometer. a. Infrared motion sensor, b UV-Vis-NIR Spectrometer, c Proximity sensor, d Integrating sphere.

3.4. Reference Laboratory Test for Measuring TSS

After the spectral acquisition from both, online and at line scanning, the samples were brought for the reference lab analysis i.e. TSS measurement. Both side of each sample was sliced longitudinally and then each side was separated into three parts: head, middle and tip as shown in Figure 3.4 (a). Pulp was squeezed directly into Digital Hand-held "Pocket" Refractometer (PAL-1 S/No L218454, Atago Japan) as shown in Figure 3.4 (b) and the distilled water was used as a calibration liquid for measuring total soluble solids. Repeat measurement was done for each part. The TSS measured from the middle part was used in model development for the offline scanning system and the average of the three parts was used for the online scanning system.

(a) (b)

Figure 3.4 (a) Sample sliced and cut into three parts (b) Mango pulp squeezed directly into the refractometer.

3.5. Outlier removal

The outliers in the reference data were identified using the following equation [92],

$$-3 \geq \frac{X_i - \overline{X}}{SD} \geq +3 \quad (3.2)$$

where, X_i is the measured value of sample i. X_i and SD are the average and standard deviation of the measured values of all samples, respectively. Sample that satisfies the equation was eliminated from data set as an outlier. From the unknown sample set the TSS value obtained outside the range of the optimum models obtained has been removed

3.6 Spectral preprocessing and model development

For offline spectroscopy, OPUS program (version 7.0.129, Bruker, Ettlingen, Germany) was used for the multivariate analysis which includes spectrum pre-processing and model development. The spectra were used for model development with and without pre-processing using the following methods: constant offset elimination, straight line subtraction, vector normalization, min–max normalization, multiplicative scatter correction (MSC), first derivatives, second derivatives, first derivatives + straight line subtraction, first derivatives + vector normalization, and first

derivatives + MSC. Partial least square regression (PLSR) multivariate technique was used to develop the model.

Similarly, for the online scanning, Realbase In-house developed program was used. Program uses Python programming language. The program followed the flowchart as shown in the Figure 3.5 for spectra acquisition. Spectra from online scanning was preprocessed using first and second order derivatives, multiple scatter correction (MSC), Min-max normalization, moving average smoothing, standard normal variate (SNV), and baseline offset.

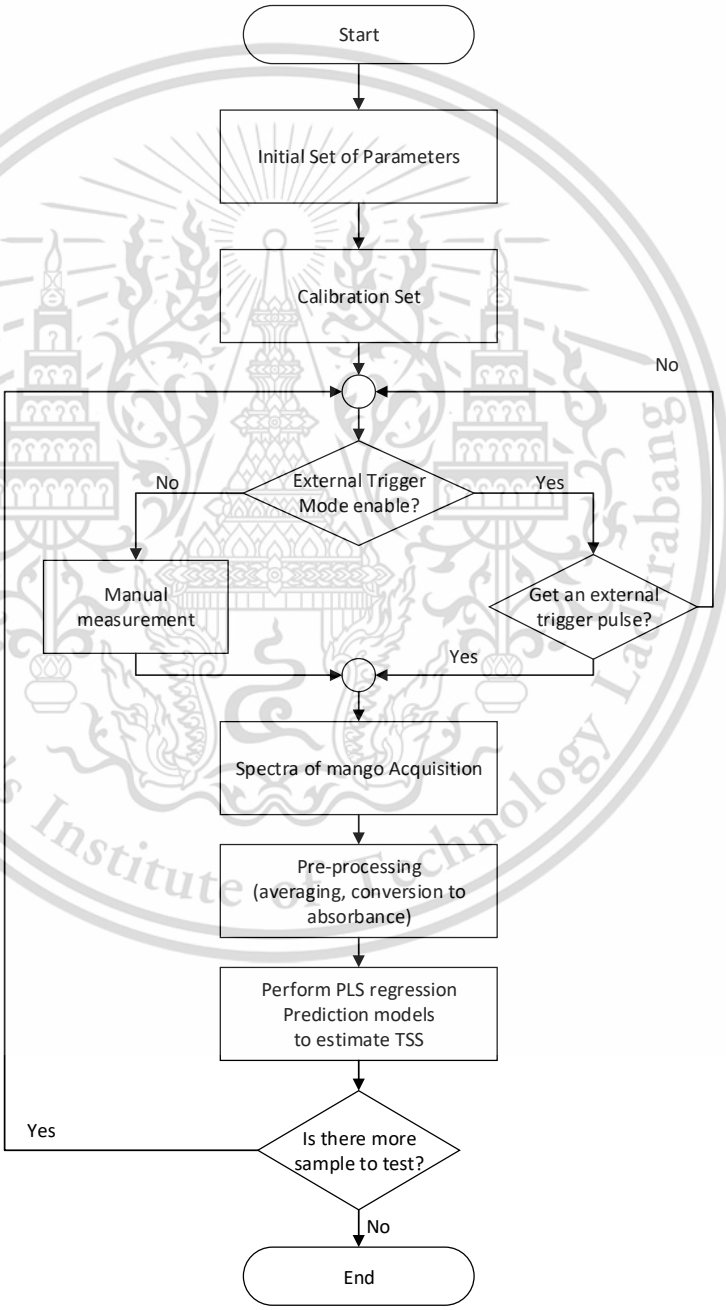

Figure 3.5 Flowchart of the Realbase In-house developed program.

3.6.1. Model for offline scanning

After the outlier removal, 182 spectra were used to establish the calibration model for both online and offline scanning condition. For offline, cross (internal) validation and test set (external) validation technique were used to develop the model. For external validation the spectra was divided into two sets: Calibration and Test sets. 80% of the total spectra was used for calibration and 20% for the test set. Thus, the model obtained by both methods were evaluated based on coefficient of determination (R^2), root mean square error of estimation (RMSEE), bias and RPD and the best model was selected with low error and high R^2 for validating the unknown sample spectra.

3.6.2. Model for Online Scanning

Same sample data set as used for developing the offline scanning model was used for online model development. Calibration model was established using the full cross validation and the performance was evaluated based on coefficient of determination (R^2), root mean square error of estimation (RMSEE), bias and RPD and the best model was selected with low error and high R^2 for validating the unknown sample spectra.

3.6.3. Sorting system for the online model validation

After selecting the appropriate model, the second part for the online scanning was for the validation using unknown samples, the mango grading system was added in the previously discussed conveying system as shown in Figure 3.6. First conveyor is equipped with the integrating sphere and UV-VIS-NIR spectrometer for scanning and the second conveyor consist of the sorting system as shown in the figure. As labeled in the picture the sample moved from station “a” to station “d”. At first, system start by placing the sample in the first station “a” which is the infrared motion sensor and as the conveyor start moving, sample passes to the spectrometer “b” for scanning. Passing through the black box, sample reaches station “c” pneumatic sticker press, where the sticker is attached to the skin of the mango and finally sorted into the three grading plates “d” according to the TSS predicted. Three plates were graded according to the TSS as “A” TSS>17 “B” TSS 15≤TSS≤17, “C” TSS<15.

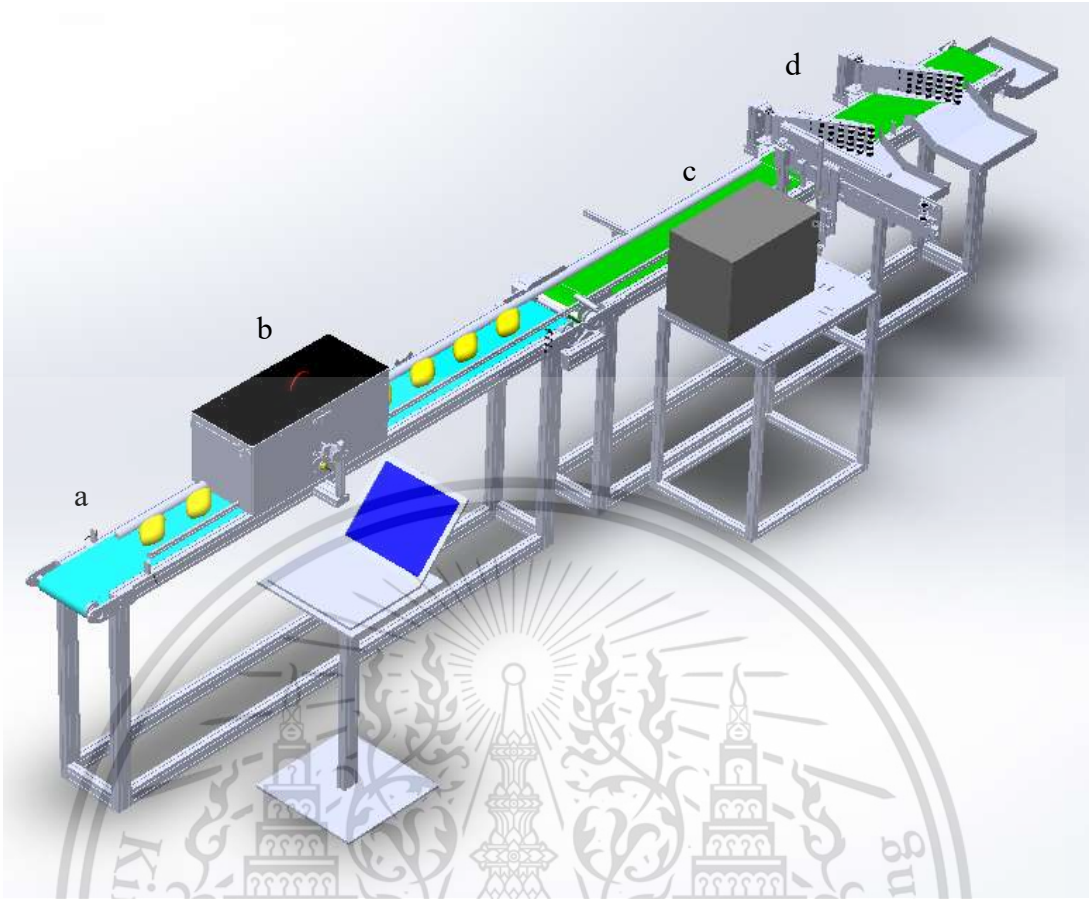

Figure 3.6 Grading and sorting online system by measuring TSS of mango.

Chapter 4

Result and Discussion

4.1 Precision test of NIR spectroscopic instrument and reference laboratory method for measuring total soluble solids of mango.

4.1.1 Repeatability and Reproducibility of instrument

Three wavenumber 10306 cm^{-1} (970nm) i.e. band of water, 6943 cm^{-1} (1440 nm) i.e. band of sucrose and 6326 cm^{-1} (1580 nm) band of starch were selected (Figure 4.1) in order to obtain the repeatability and reproducibility for offline scanning by Fourier Transform NIR spectrometer. Similarly the wavelength selected for the online scanning by fiber optics spectrometer were 760 nm [45] i.e. band of water, 680 nm [93] i.e. band of chlorophyll, 913 nm i.e. band of sucrose [45] (Figure 4.2).

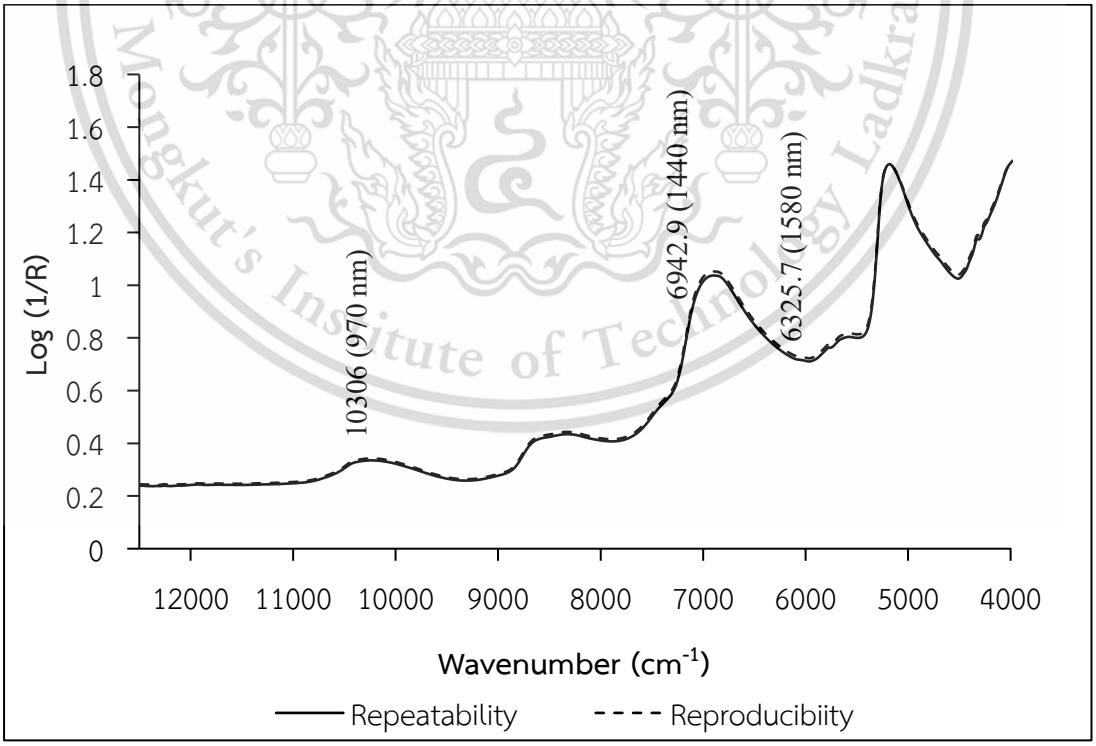

Figure 4.1 Average Spectra from Offline Scanning.

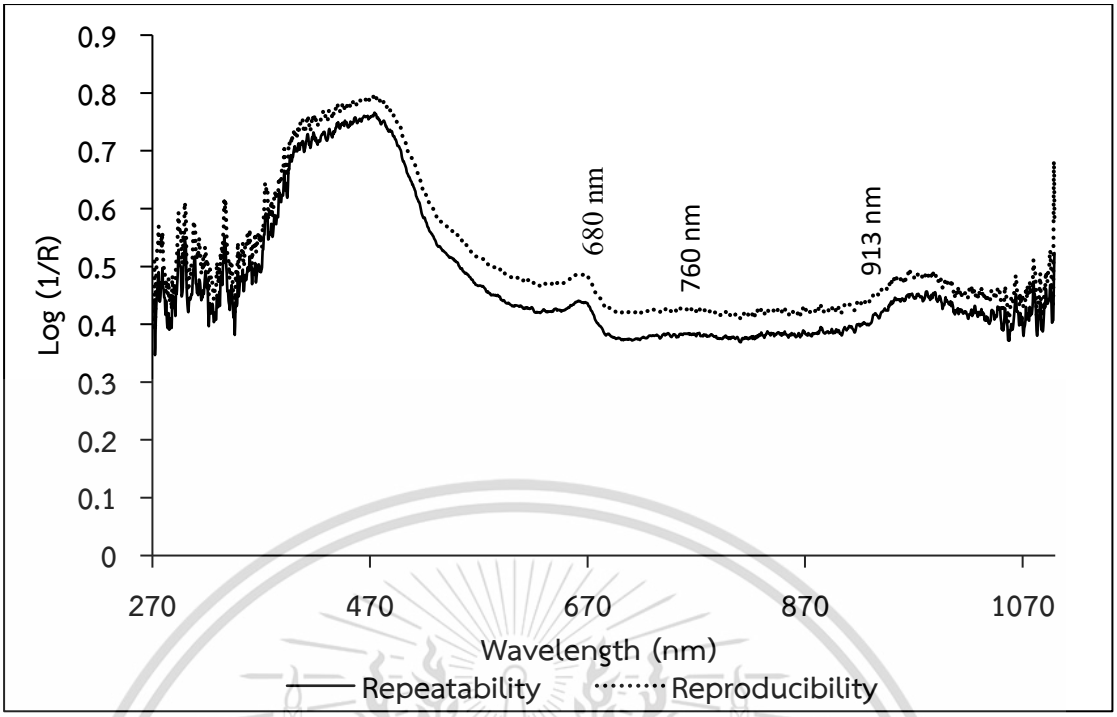

Figure 4.2 Average Spectra from Online Scanning.

Table 4.1 Spectral repeatability and reproducibility by online and offline scanning.

Scanning	Repeatability	Reproducibility
Online	0.00419	0.032041
Offline	0.000775	0.008262

The mean absorbance value of the repeatability and reproducibility of offline scanning instrument was obtained to be 0.632 and 0.675. Similarly, mean absorbance value of the repeatability and reproducibility of offline scanning instrument was obtained to be the offline and online scanning instrument was obtained to be 0.472 and 0.514, respectively. From Table 1 it was observed that the repeatability and reproducibility of offline scanning is low, 0.000775 and 0.008262. Repeatability is the variation caused by the instrumentation or the variation observed when the same operator measures the same part more times with the same instrumentation. Reproducibility is the variation caused by the measurement system or the variation observed when different operators measure the same part with the same instrumentation [94]. Reproducibility indicates the homogeneity of the sample. Low repeatability value means low variation between the measurements that indicate

highly repeatable and precise scanning instrument. More robust model can be expected from offline scanning instrument [95]. There are many parameters that should be considered in online scanning conditions. Parameters such as the surface roughness of the sample, the average distance from the sample to the optics are parameters that can also significantly influence the quality, repeatability and reproducibility of the spectra generated [96]. To obtain robust models for NIR spectroscopy applications with an acceptable level of accuracy and precision, it is essential to set up the optimal operational conditions to assess the adequate online measurement [85].

4.1.2 Precision of Reference Laboratory

Table 4.2 shows the TSS measured for three sample to obtain the repeatability. Repeatability of reference data was calculated 0.1403. $\mathbf{R^2_{Max}}$ was obtained to be 0.967. R^2_{Max} is possible only when there is no error in the spectra or model [97]. The error from reference method was found to be 3.3% and with the accuracy value of 96.7%. It was concluded that it is possible to develop NIR model using total soluble solids.

Table 4.2 Total soluble solids measured by reference laboratory.

No of Sample	Tip			Middle			Head		
1	18.3	18.4	18.4	17.3	17.4	17.5	18.6	19.0	19
2	17.9	18.0	18.1	18	17.9	17.8	19.9	19.5	19.8
3	21.1	21.1	21.0	19.9	20.0	20.1	20.8	21.1	20.7

4.2. Model from Offline Scanning

4.2.1 Spectral Analysis

In order to analyse the spectral characteristic obtained by offline scanning using full wavelength spectrometer, the spectra is averaged as shown in the Figure 4.3.

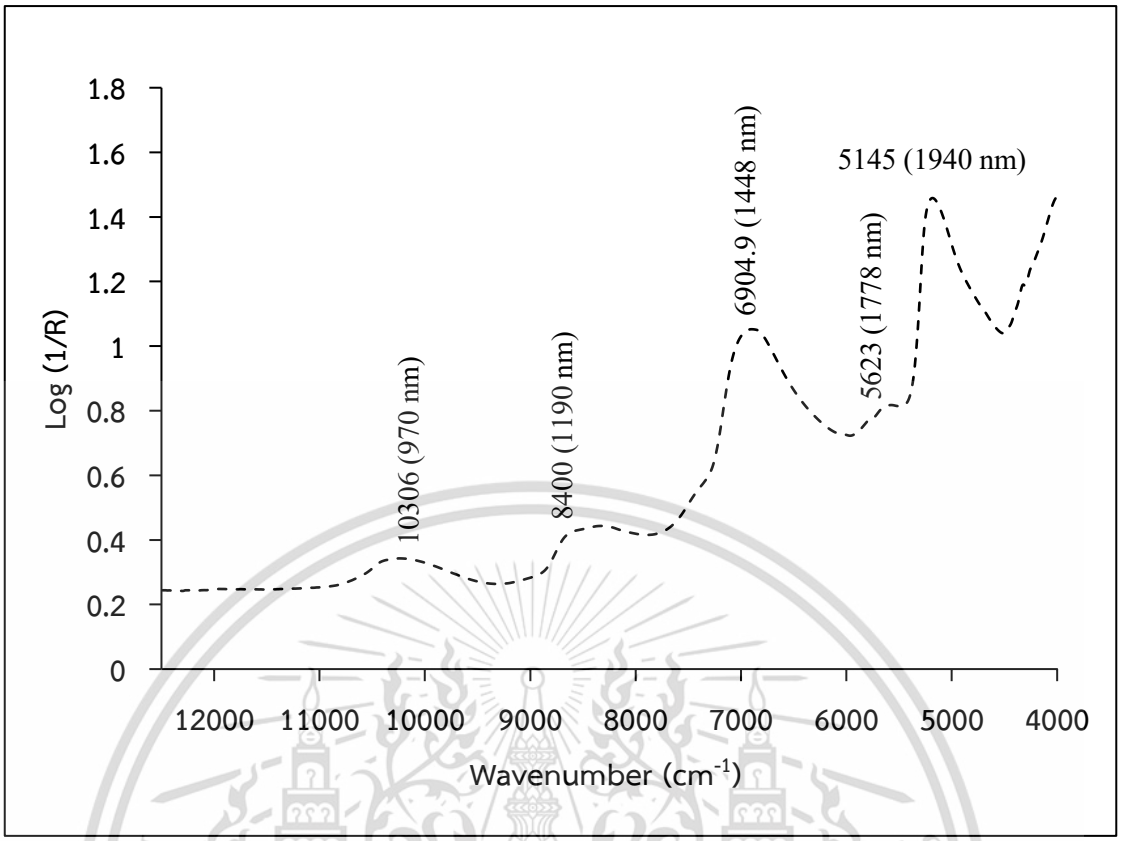

Figure 4.3 Average raw absorbance spectra obtained from offline scanning.

The Figure 4.3 displays the peaks at 10306 cm^{-1} (970 nm), 6942.9 cm^{-1} (1440 nm), 5623 (1778 nm) and 5145 cm^{-1} (1940 nm). The peak at 10306 cm^{-1} (970 nm) is due to absorption band of the second overtone associated with O-H stretching of H_2O and C-H overtone region associated with sugar, at 6908.9 cm^{-1} (1448 nm) is the absorption band associated with the first overtone O-H stretching of water and starch [45], at 5623 cm^{-1} (1778 nm) is the absorption band corresponding to the (1780 nm) first overtone of C-H stretching of cellulose and can be related to the sugar [45] and at 5145 cm^{-1} (1940 nm) is the absorption band of the second overtone associated with O-H stretching and O-H bending combination of H_2O [45]. According to the Delwiche et al. [33], the sugar absorption band generally arising from second or third overtone of Oxygen-hydrogen (O-H) stretched and third and fourth overtone of Carbon-Hydrogen (C-H) occur near strong dominating water absorption region in the fruits containing high amount of water such as mango.

4.2.2. Total soluble solids prediction using partial least squares regression for offline condition

The mean, max, min and SD of the Total soluble solids (TSS) measured in the sample using the reference method has been listed in the Table 4.3. Figure 4.5 shows the normal distribution of TSS measured using the standard refractometer analysis. From the Figure 4.5, it was observed that the TSS measured for model development had the normal distribution ranging from 14 to 20%. In order to confirm the normal distribution a normal quantile-quantile (Q-Q) plot is shown in Figure 4.6. In Figure 4.6 as the data falls in the reference straight line, it implies that data set obtained has the normal distribution. Also from the Q-Q plot we can observe any outliers presented in the data set. As the TSS was measured from the head to the tip of the mango it was observed that the TSS content in the head part was appeared to be higher and gradually decreased towards the tip. The standard deviation between the parts of sample measured (head, middle and tip) was obtained to be approximately between 0.5 to 2%.

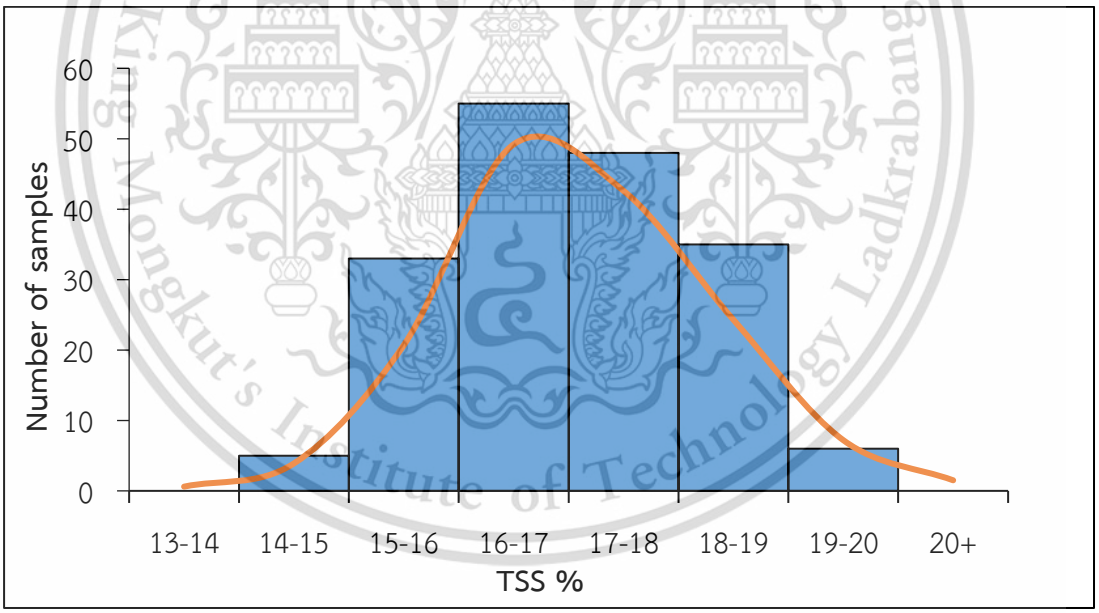

Figure 4.4 Histogram representing TSS measured using the reference method for model development.

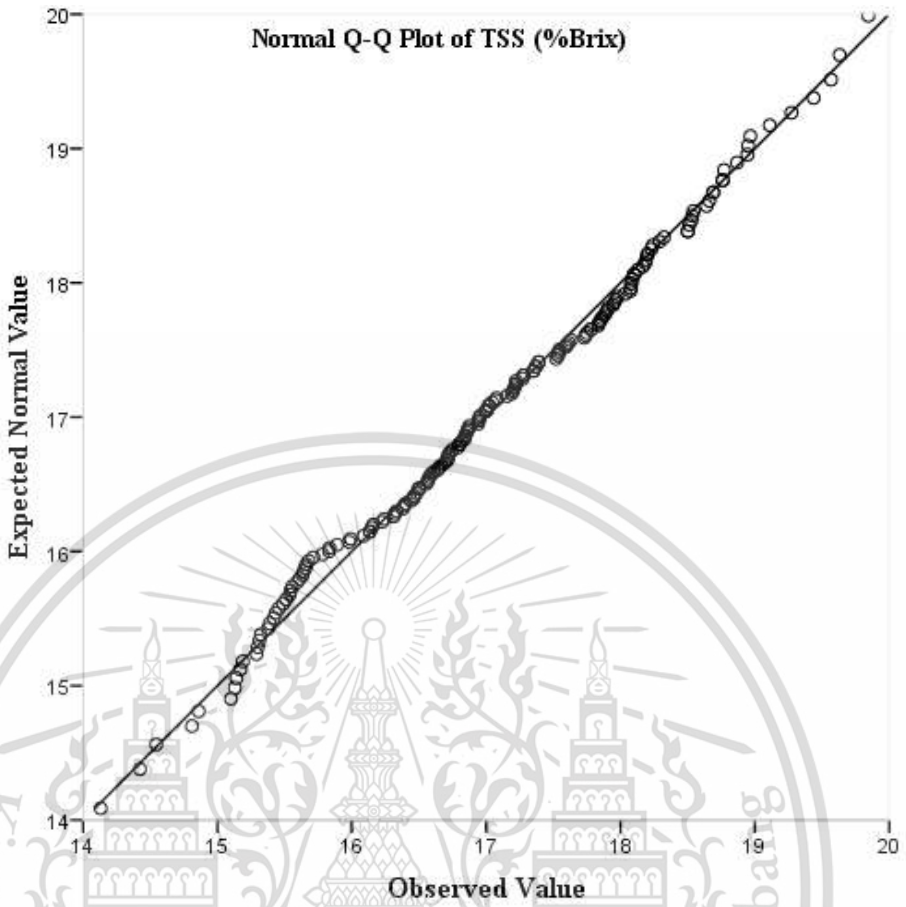

Figure 4.5 Normal Q-Q plot representing the data set.

Table 4.3 Total soluble solids of mango measured by reference laboratory used for model development by offline scanning and validation.

Model	Calibration					Test				
	N	Mean (%)	Max (%)	Min (%)	SD (%)	N	Mean (%)	Max (%)	Min (%)	SD (%)
Offline (Cross Validation)	182	16.8	20.1	13.3	1.3					
Offline (Test Set) Validation)	146	16.75	20.1	13.3	1.21	36	17.01	19.9	13.9	1.6

where, N is the number of sample, Max is maximum value, Min is the minimum value and SD is the standard deviation.

Table 4.4 Results of the PLS calibration models for the Offline data using cross validation.

Model	Preprocessing	Spectral Range	Factor	Calibration				
				R^2	RMSEE (%)	r^2	RMSECV (%)	RPD
NIR	Straight line Subtraction	9403.8-6094 5454-4242.9	8	0.70	0.729	0.64	0.776	1.67

Table 4.5 Results of the PLS calibration models for the Offline data using test set validation.

Model	Preprocessing	Spectral Range	Factor	Calibration				
				R^2	RMSEE (%)	r^2	RMSEP (%)	RPD
NIR	No preprocessing	9403.8-6094 5454-4242.9	10	0.67	0.721	0.83	0.645	2.46

Table 4.4 and 4.5 shows the result of PLS regression model for offline scanning condition using full cross and test set validation technique The coefficient of determination (R^2), root mean square error of estimation (RMSEE), residual prediction deviation (RPD) and bias has been shown in the table. The optimum model was selected based on the statistical data. Model developed using the interactive NIR range with straight line subtraction preprocessing provided the best result. Figure 4.7 shows the scatter plot of measured TSS versus predicted TSS in the mango by using offline scanning condition of calibration and test set.

Figure 4.8 shows the regression coefficient plot of the optimum model for the TSS content of mango. The band relevant to the prediction of TSS content has been revealed in the figure.

The band appeared in the regression coefficient plot reveal that most of the absorption band arise from the overtone and combination of C-H stretch. The band structure and details are described in the Table 4.6. The X-loading weight plot for the prediction of the TSS content is shown in Figure 4.9. The highest peak in the graph indicates the corresponding wavelength has the highest influence in the prediction of TSS content.

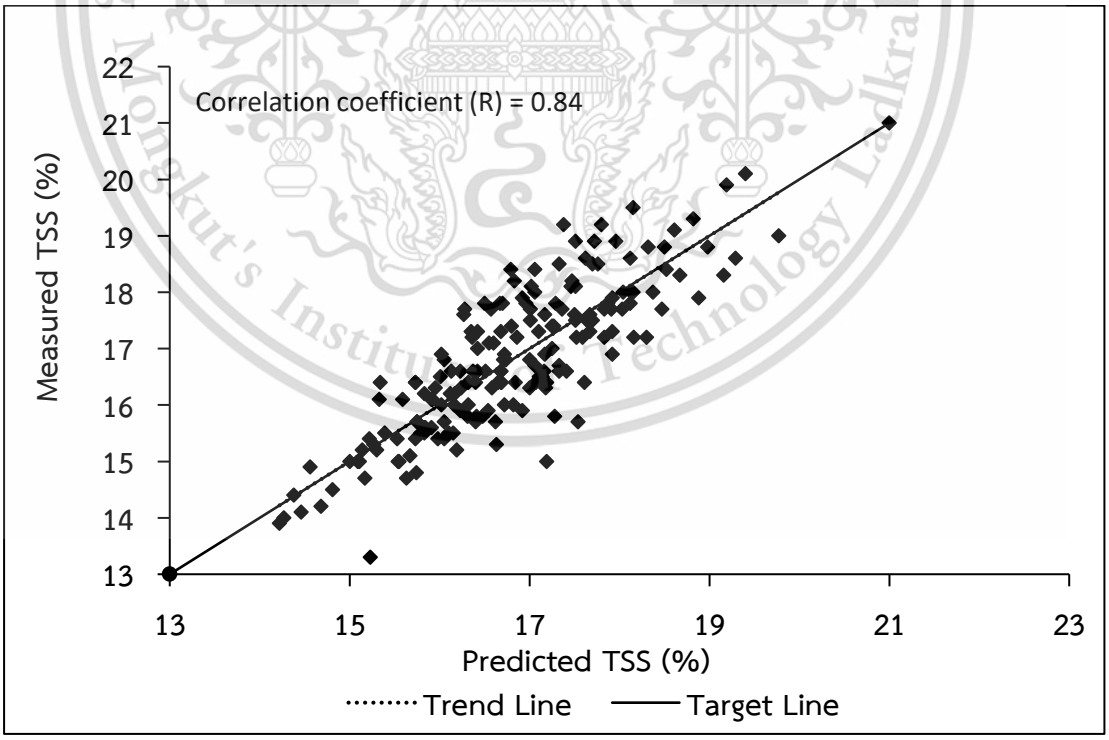

Figure 4.6 Scatter plot of Predicted TSS content with Measured TSS in calibration data set.

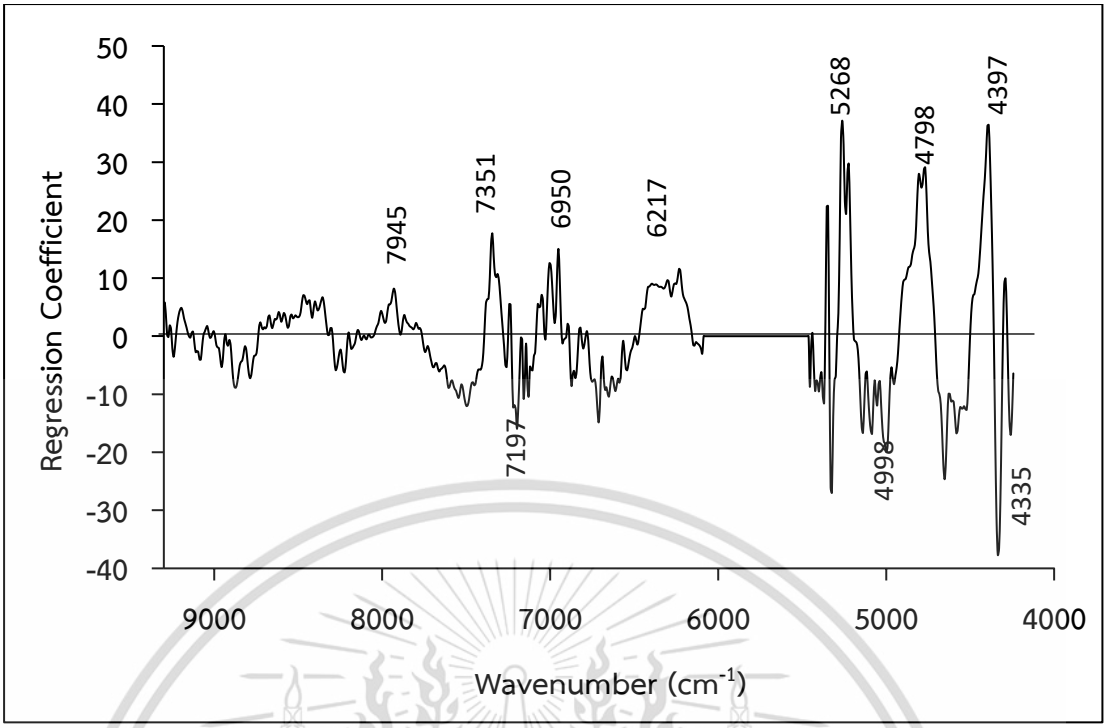

Figure 4.7 Regression coefficient plot of optimum model for TSS content in mango by Offline scanning.

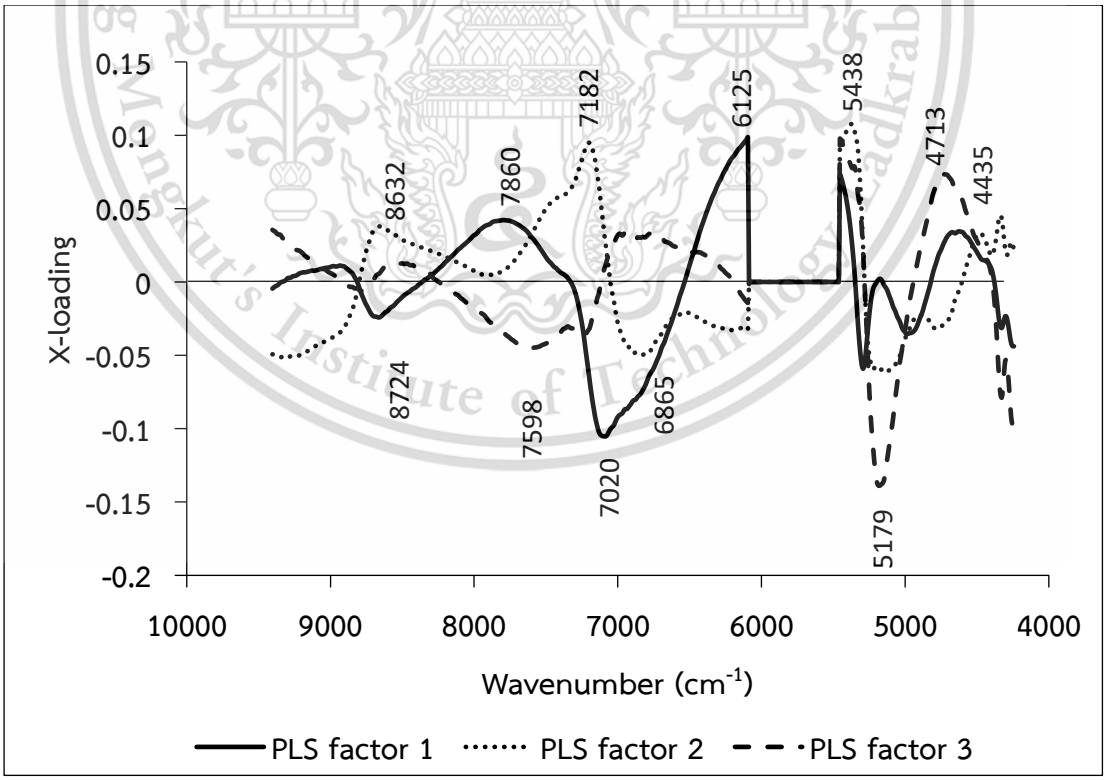

Figure 4.8 X-loading weight plot of optimum model for TSS content in mango by offline scanning.

Table 4.6 Vibration band of the peak appeared in the regression coefficient plot in the offline experiment.

Wavenumber (cm^{-1})	Wavelength (nm)	Wavelength (nm) Referred from reference	Bond vibration	Structure
7495	1258	1225	C-H str. second overtone	CH[45]
7351	1360	1360	2*C-H str + C-H def	CH_3[45]
7197	1389	1395	2*C-H str + C-H def	CH_2[45]
6950	1438	1440	O-H str First Overtone	Sucrose[45]
6217	1608	1620	C-H str. First overtone	$=CH_2$[45]
5268	1898	1900	O-H str.+ 2*C-O str	Starch[45]
4998	2000	2000	2*O-H def + C-O def	Starch[45]
4798	2084	2080	O-H str + O-H def	Sucrose[45]
4335	2306	2310	C-H str + C-H def	CH_2[45]
4397	2274	2280	C-H str + C-H def	CH_3[45]

Table 4.7 Vibration band of the peak appeared in the X-loading plot in the offline experiment.

Wavenumber (cm^{-1})	Wavelength (nm)	Wavelength (nm) Referred from reference	PLS Factor	Bond vibration	Structure
4435	2254	2252	2	O-H str + O-H def	starch[45]
5179	1930	1940	2,3	O-H str + O-H def	H_2O [45]
5438	1838	1820	1,2,3	O-H str+2*C-O str	cellulose[45]
6125	1632	1620	1	C-H str. First overtone	CH_2[45]
6865	1456	1450	2	O-H first overtone	H_2O,starch[45]
7020	1424	1440	1	O-H str First Overtone	Sucrose[45]
7598	1316	1225-1360	3	C=H str. Second overtone and combinational	CH, CH_3[45]
8724	1146	1152	1	C-H str. second overtone	CH_3[45]
8632	1158	1152	2	C-H str. second overtone	CH_3[45]
7182	1392	1395	2	2*C-H str + C-H def	CH_2[45]

The Table 4.6 and 4.7 gives the list of the vibration band appeared in regression and X-loading plot. Table shows that the highest peaks appeared in both regression and X-loading plot are the peak associated with sucrose and starch are revealed. The peaks around 6950 cm^{-1} (1440 nm) in the regression coefficient plot assigned as the bond vibration of O-H str First Overtone of sucrose according to Osborne et al. [45].

Similarly the absorption band 4798 cm^{-1} (2080nm) reveled the vibration band O-H str + O-H def of sucrose as well. The dominating peak in the regression plot is due to the C-H stretch overtone or combination band which could be indicated as the important peak for TSS prediction in Mango. The peak from 6900-7200 cm^{-1} (1449-1380 nm) in the X-loading plot assigned as the bond vibration of O-H str First Overtone X-loading plot is explained by the PLS factor 1, which is considered as the important peak for the prediction of TSS. Similar dominant absorption appeared in the X-loading plot is assigned as the vibration peak of sucrose, starch and water. These peaks show the influence of absorption bands on the prediction of TSS in mango.

The optimum model selected was used to predict the unknown set of sample. 106 samples were scanned using the offline condition. TSS was predicted by using the selected model developed by PLS regression. Table 4.8 shows the statistical value of prediction by using the optimum model with lowest PLS factor with R^2 (0.70) and RMSEE (0.729%). Figure 4.10 shows the scatter plot of measured with predicted TSS using selected PLS model.

Table 4.8. Total soluble solids measured by reference laboratory for unknown samples to validate model obtained by offline scanning.

	N	Mean (%)	Max (%)	Min (%)	SD (%)
Unknown set	106	17.9	20.1	15.0	1.2

Table 4.9 Statistical data for TSS prediction in unknown sample set using the selected PLS model.

N	SEP (%)	RPD	Bias (%)	Offset	Slope
106	0.97	1.27	1.57	5.126	0.626

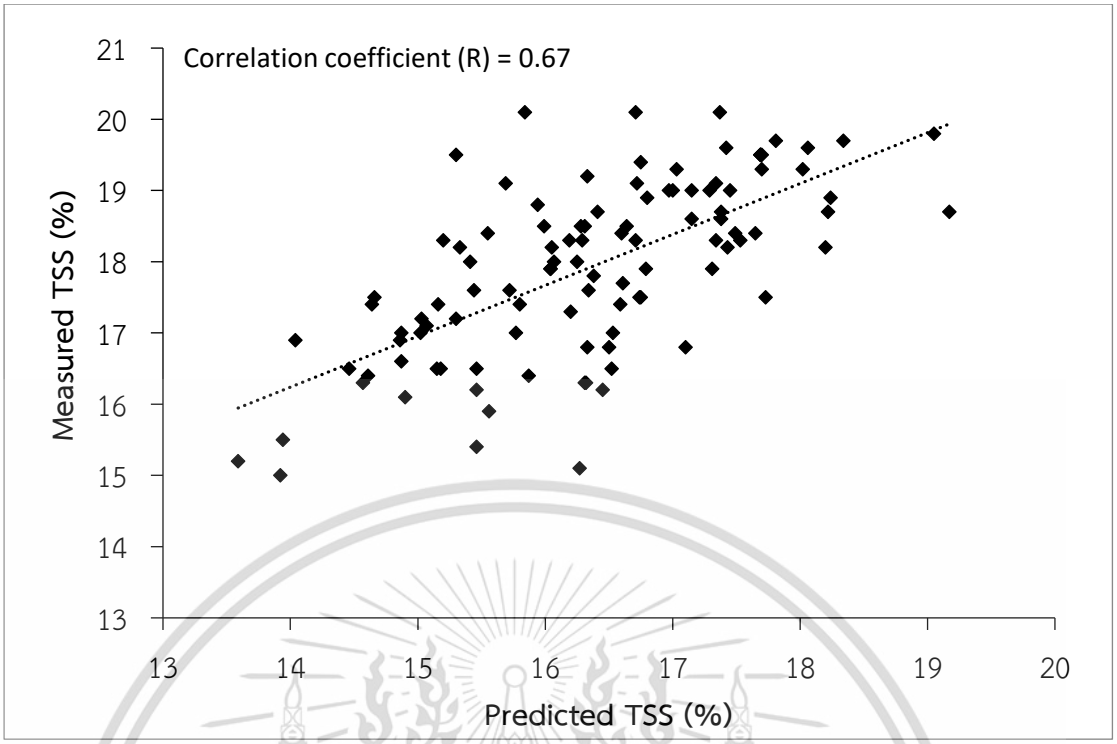

Figure 4.9 Scatter plot of measured with predicted of TSS in the unknown set of sample.

Table 4.8 shows the statistical value of TSS measured by reference laboratory for unknown sample set. Table 4.9 shows the standard error of prediction 0.97% and bias 1.57% when the calibration model is used to predict the TSS of unknown sample. However, from the literature review, research based on the evaluating the TSS of mango using NIRS the result obtained is comparable. According to Nordey et al. [97], lower prediction errors were obtained for the TSS content (RMSEC = 0.60°Brix and RMSEP = 0.89°Brix) [98-101]. The authors of these studies reported standard errors of prediction (SEP) and root mean square errors of prediction (RMSEP) that varied from 0.55 to 1.45°Brix. Thus the model obtained by offline scanning using FTNIR spectroscopy for measuring TSS of mango with R^2 from 0.66-0.81 can be considered for the rough screening and some other approximate calibrations according to Williams, 2007 [44].

4.3 Model from Online Scanning

4.3.1 Spectral Analysis

The Figure 4.11 shows the raw spectra obtained using the online scanning condition. The range used to develop the model was from 600-1000 nm. As observed no any significant absorption band was noticed in the raw spectra. Figure 4.12 shows the preprocessed spectra using moving average smoothing segment of 21 points in combination with the multiple scatter correction.

In Figure 4.12 upward valleys has been notices in the spectra at 760 nm and 980 nm which are assigned as the absorption band of water. The absorption band in 760 nm and 980 nm is also considered as band of sucrose in water due to O-H stretching of second and third overtone according to Golic et al. [102]. The absorption bands observed in the SWNIR spectra is moreover relevant for predicting the TSS in mango as it can reveal overtone and combination band of OH and CH group related to the sucrose in water [102]. As observed in the figure, few absorption peaks are noticed in the range of 600-1000nm.

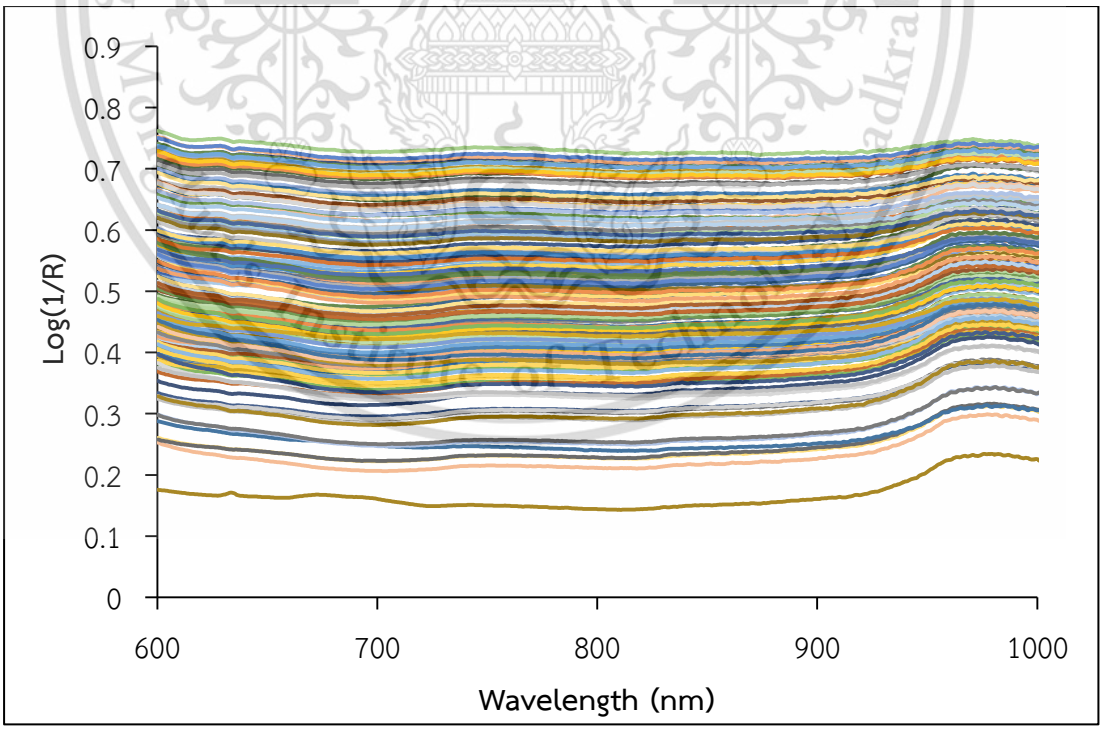

Figure 4.10 Raw spectrum obtained from the online scanning condition.

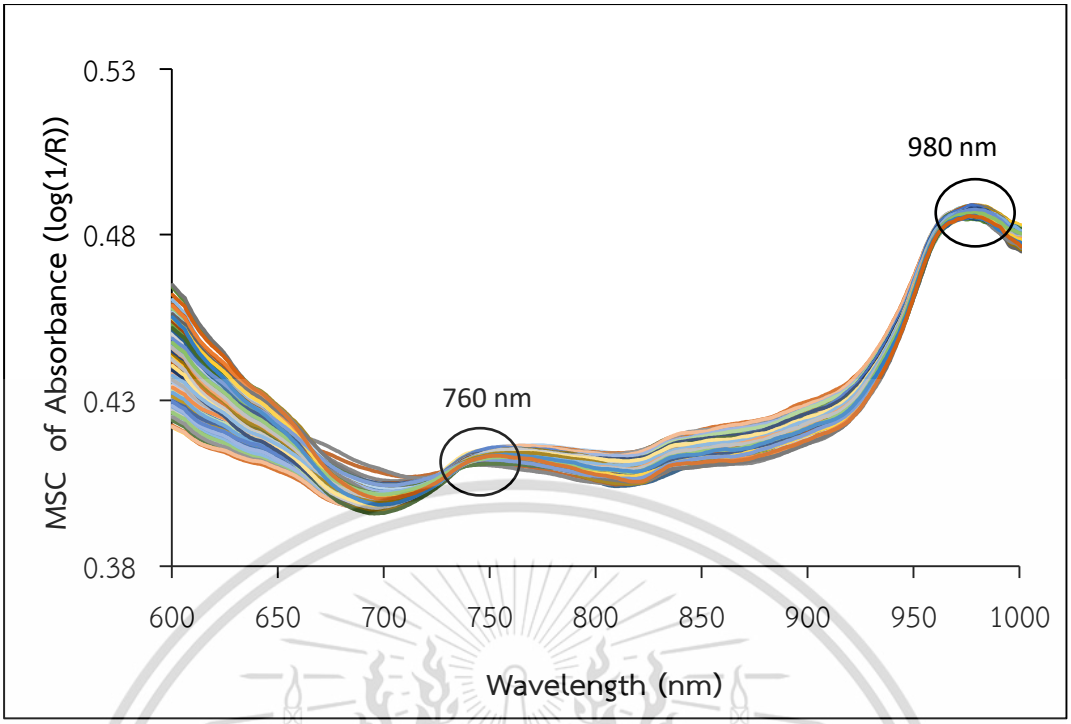

Figure 4.11 Preprocessed spectra using moving average smoothing and multiple scatter correction.

4.3.2 Total soluble solids prediction using partial least squares regression for online condition

Table 4.10 shows the statistical data of TSS measured by reference laboratory analysis. Mean, max, min and standard deviation was calculated. Similarly Table 4.11 shows the result of PLS regression for developing the calibration model using online scanning condition. Moving average smoothing in combination with Standard Normal Variate, Multiple Scatter Correction and Mean Normalization was used to develop the model. Based on the statistical values of R^2, RMSEC and the lowest PLS factor used, the optimum model for prediction was selected. Thus, the model was used for further prediction of TSS in mango using the unknown set of sample.

Table 4.10 Total soluble solids of mango measured by reference laboratory used for model development by online scanning and validation.

Model	Calibration				
	N	Mean(%)	Max(%)	Min(%)	SD(%)
Online scanning	182	17.04	19.8	14.3	1.16

Table 4.11 Results of the PLS calibration models for the online data using cross validation.

Model	Preprocessing	Factor	Calibration		Validation		
			R^2	RMSEC	r^2	RMSECV	Bias
1	Moving Average Smoothing+ SNV	6	0.60	0.7271	0.53	0.7983	0.00365
2	Moving Average Smoothing+ MSC	6	0.61	0.7256	0.54	0.7927	0.01364
3	Moving Average Smoothing+ Mean Normalization	7	0.60	0.7300	0.53	0.7993	0.00076

From the result obtained in the Table 4.10 model number 2 with pretreatment of moving average smoothing using 21 segments combination with MSC was selected as the optimum model of calibration. Though the results shows not much significant difference between the pretreatment used, but based on the number of factor used and the error of calibration the model was selected. Figure 4.13 shows the scatter plot of the measured versus predicted TSS of the calibration set. Figure 4.14 shows the regression coefficient plot of the best model for measuring TSS in mango for online condition. Similarly, Figure 4.15 shows the x-loading plot of the best model obtained for online scanning. The peaks that are observed in both regression and x-loading plot are mainly the band associated with chlorophyll and sucrose.

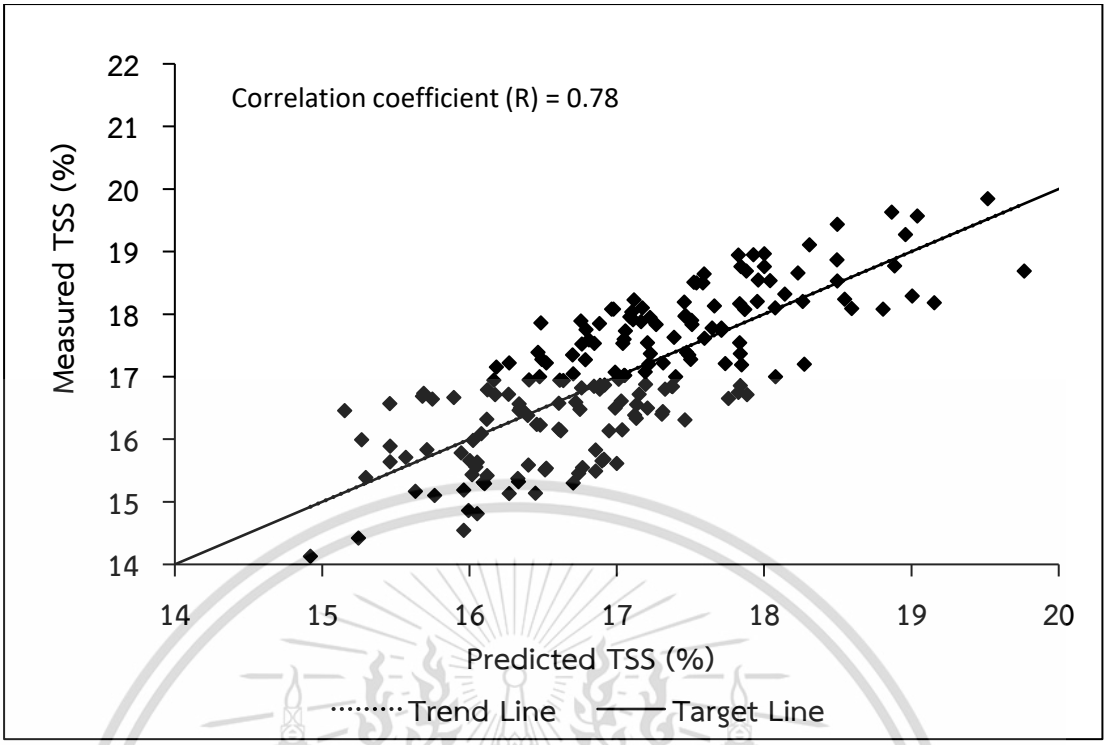

Figure 4.12 Scatter plot of Predicted TSS content with Measured TSS in calibration data set.

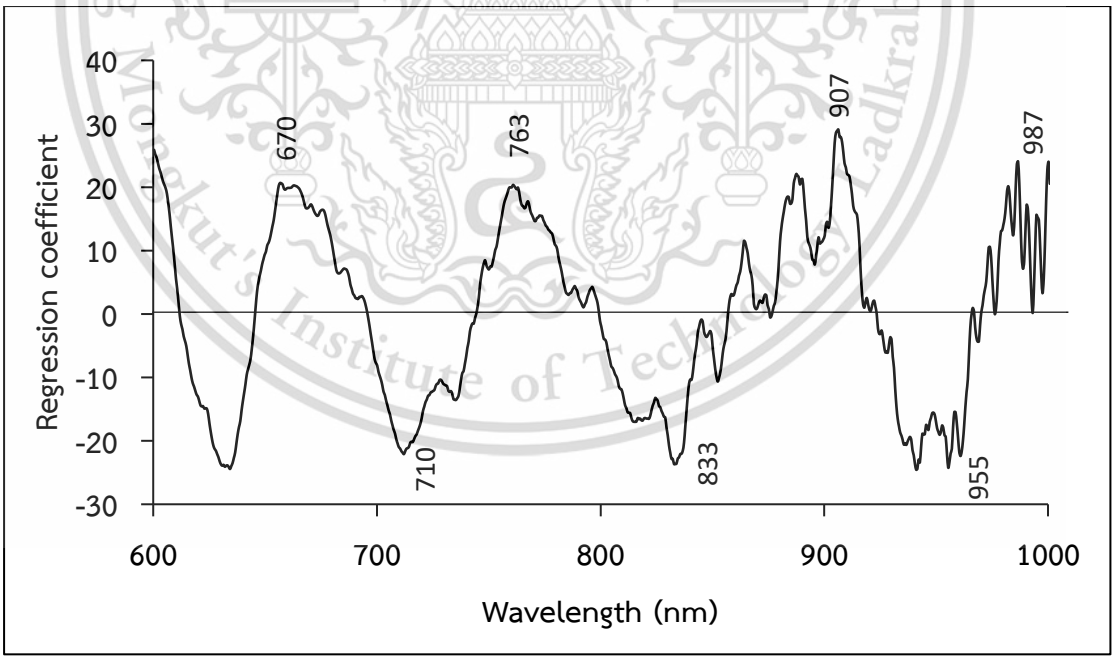

Figure 4.13 Regression coefficient plot of optimum model for TSS content in mango by online scanning.

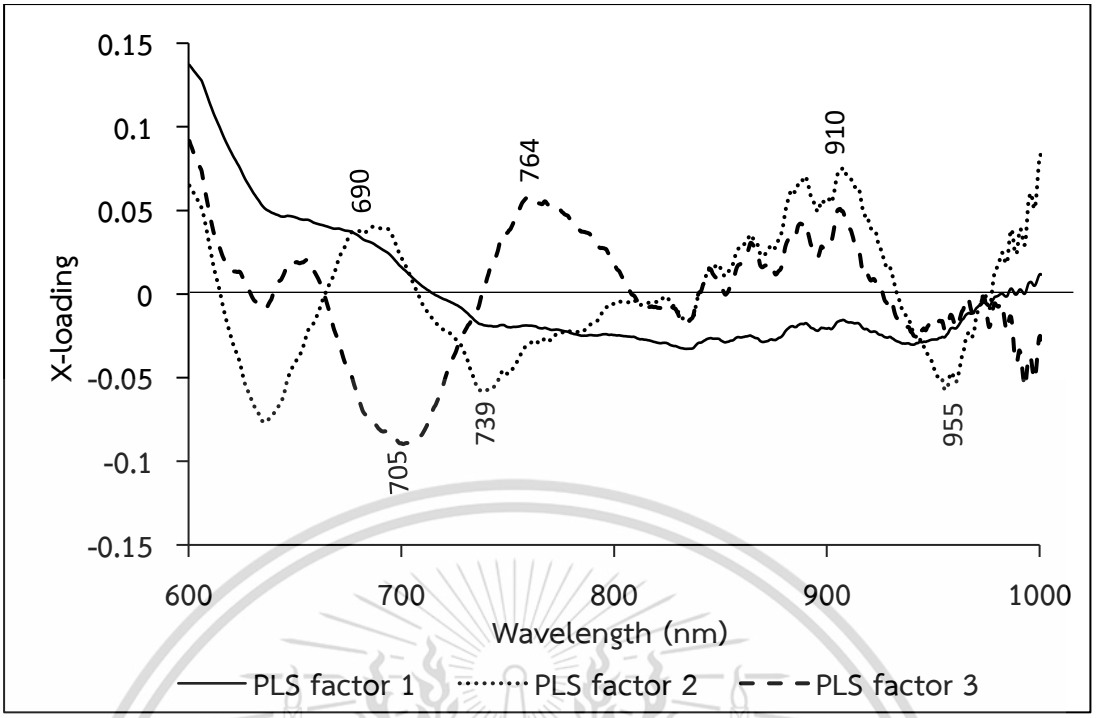

Figure 4.14 X-loading plot of optimum model for measuring TSS content in mango by online scanning

The highest peaks observed in the regression plot is the shifted peak of chlorophyll at around 670 nm and the shifted peak around 907 nm which is the vibration band of O-H str. third overtone of sucrose. Similarly the peak around 763nm is assigned as the bond vibration of O-H str third overtone of sucrose by Golic et al, [102]. Vibration band around 833 nm is the shifted peak of O-H combination of sucrose. Table 4.12 shows the vibration band of the peak appeared in the regression plot obtained from the model obtained from online scanning. The peak around 764 nm and 910 nm in the X-loading plot assigned as the bond vibration of O-H str third overtone and C-H str. third overtone of sucrose in X-loading plot is explained by the PLS factor 2 and 3, which is considered as the important peak for the prediction of TSS. Table 4.13 shows the vibration band of the peak appeared in the X-loading plot obtained from the model. These band has the highest influence in the prediction of TSS in the model obtained by online scanning.

Table 4.12 Vibration band of the peak appeared in the regression plot obtained from online scanning

Wavelength (nm)	Wavelength (nm) Referred from reference	Bond vibration	Structure
670	680		Chlorophyll[98]
763	770	O-H str Third Overtone	Sucrose[102]
833	840	O-H Combination	Sucrose[102]
907	910	C-H str Fourth Overtone	Sucrose[102]
955	960	O-H str Second Overtone	Sucrose[102]
987	984	O-H str Second Overtone	Sucrose[102]

Table 4.13 Vibration band of the peak appeared in the X-loading plot obtained from online scanning.

Wavelength (nm)	Wavelength (nm) Referred from reference	PLS Factor	Bond vibration	Structure
690	680	2		Chlorophyll[98]
739	740	3	O-H str. Third overtone	Sucrose[102]
764	770	2	O-H str Third Overtone	Sucrose [102]
910	910	2,3	C-H str. Third overtone	Sucrose[102]
955	960	1,2,3	O-H str Second overtone	Sucrose[102]

Table 4.14 shows the statistical value of TSS measured by using reference laboratory for unknown sample set. The optimum model selected was used to predict the unknown set of sample. Table 4.15 shows the statistical data for TSS prediction in unknown sample set using the selected PLS model. SEP reported to predict the TSS of unknown set is 1.24% and the bias is -1.06% which is comparatively higher than that

of offline condition. Figure 4.16 shows the scatter plot of measured with predicted value of TSS in the unknown set of sample.

Table 4.14 Total soluble solids measured by reference laboratory for unknown samples to validate model obtained by online scanning.

	N	Mean (%)	Max (%)	Min (%)	SD (%)
Unknown set	95	18.0	19.8	14.9	1.2

Table 4.15 Statistical data for TSS prediction in unknown sample set using the selected PLS model.

N	SEP (%)	RPD	Bias (%)	Offset	Slope
119	1.24	1.02	-1.06	10.34	0.37

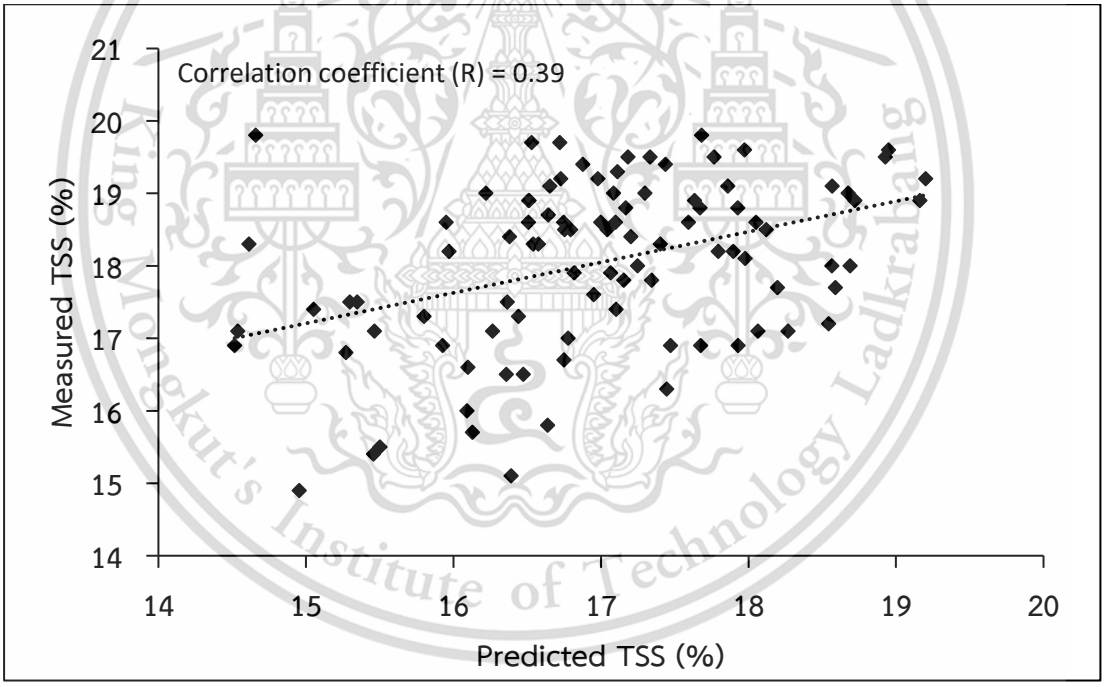

Figure 4.15 Scatter plot of Measured with predicted of TSS in the unknown set of sample.

Several parameters are responsible for high SEP during the TSS measurement using online scanning condition. Focal length, integration time, speed can be considered as the main source of error. Since, the size of the sample was not uniform so focal length changes per sample. Similarly, while scanning in motion the noise in the spectrum is due to the conveying system which cannot be eliminated completely.

Also, because of the highly non homogeneous nature of Mango, TSS couldn't be predicted precisely while in motion. As a consequence of these problem the SEP was obtained to be higher while scanning in online system compared to the offline scanning condition.

Chapter 5

Conclusion

The raw spectra obtained by whole NIR range FT-NIR spectrometer reveal some dominant peak of water and starch, whereas, the raw spectra obtained by using short wave diode array spectrometer did not reveal any significant peak. But, after preprocessing the raw spectra obtained by using the online condition, the dominant valley represented the vibration band of sucrose, which was considered as important peak. The spectra acquired by offline scanning was smooth without noise as the sample was at rest, at the same time the spectra attained by online scanning during the motion contain noise which was further reduced by smoothing preprocessing techniques. The preprocessed or raw spectra obtained by both condition using online and offline condition were informative and reveal most of the peak related to TSS content in mango.

The total soluble solids content prediction model developed from the spectra obtained by the online scanning using short wave diode array spectrometer shows the effect of noise from the system and error due to the change in focal length. Although the error was slightly greater compared to the offline condition but the regression plot revealed most of band associated with sucrose had the high influence in the prediction of the TSS. Model obtained by online scanning can be used for the rough screening. From the result it can be concluded that it is feasible to use short wave fiber optic spectrometer for measuring the TSS in mango for sorting the fruit in the firm.

Models obtained by both online and offline scanning conditions were comparable. The root mean square error of model from FT-NIR spectrometer is slightly lower than the diode array spectrometer. But optimum PLS factor used for the development of calibration model for offline scanning is higher than that of the model developed from the online scanning. Low PLS factor is recommended for the model development using NIR spectroscopy. From this research, it can also be concluded that the model obtained using the online scanning system contain high error percentage because of the highly non homogeneous nature of mango. The size and the shape of Mango has to be considered for online scanning. Different fruits has been analyzed using both scanning condition by NIR spectroscopic techniques. But the real time analysis is more important considering the present demand than analyzing in lab condition.

5.1 Recommendation

As a recommendation, further research on reducing the error percentage in suitable way should be done in order to develop the robust model using the diode array fiber optics spectrometer for the online condition. As from this research it can be concluded that it is feasible to use NIR spectrometer for online scanning, so further model can be developed for measuring other quality attributes for highly exported agricultural products.

References

[1] Thai Custom (2018, September). [Online]. Available: http://www.customs.go.th/statistic_report.php?lang=en&show_search=1 2018.

[2] Siddiq, M., Brecht, J.K., Sidhu, J.S. (2017). Handbook of Mango Fruit: Production, Postharvest Science, Processing. The Atrium , Southern Gate, Chichester, West Sussex , PO19 8SQ, UK. Wiley Publication.

[3] Brennan, D., Alderman J.; Sattler L., O'Connor, B., O'Mathuma, C. (2003). Issues in development of NIR micro spectrometer system for on-line process monitoring of milkproduct. Measurement. 33, pp. 67–74.

[4] Huang, H., Yu, H., Xu, H., Ying, Y. (2008). Near Infrared Spectroscopy for On/In line monitoring of quality in food and beverages: A review. Journal of Food Engineering. 87(3), pp. 303-313.

[5] Pemen, A.J.M., van der Laan, P.C.T., Kema, A. (1998). On-line detection of partial discharges in statorwindings of largeturbine generators. IEE colloquium on discharges inlarge machines. pp 3/1–3/4.

[6] Sirisomboon P., Kaewkuptong A., Williams P. (2013). Feasibility study on the evaluation of the dry rubber content of field and concentrated latex of Para rubber by diffuse reflectance near infrared spectroscopy. Journal of Near Infrared Spectroscopy. 21, pp. 81–88.

[7] Andersson, M., Svensson, O., Folestad, S., Josefson, M., Wahlund, K.G. (2005). NIR spectroscopy on moving solids using a scanning grating spectrometer—impact on multivariate process analysis. Chemometrics and Intelligent Laboratory Systems. 75, pp. 1-11.

[8] Farnandez- Ahumada, E. (2008). Assessment of the potential of Near Infrared Reflectance Spectroscopy to be implemented in the feed manufacturing industry for process control. PhD Dissertation. University of Cordoba.

[9] Sanchez, J. A. C. (2012). Using NIRS spectroscopy to predict postharvest quality. [Online]. Available: http://digital.csic.es/bitstream/10261/52943/4/Using_NIR.pdf.

[10] Riquelme, M.T. (2008). Transmisión óptica e imagen en visible e infrarrojo en frutas. Ensayo de equipos comerciales. Doctoral thesis. Universidad Politécnica de Madrid

[11] Bellon, V., Vigneau, J.L., Sevilla, F. (1994). Infrared and near-infrared technology for the industry and agricultural uses: on-line applications. Food Control. 5, pp. 21-7.

[12] Huang, H., Yu, H., Xu, H., Ying, Y. (2008). Near infrared spectroscopy for on/in-line monitoring of quality in foods and beverages: a review. Journal of Food Engineering. 87, pp. 303-13.

[13] Rodríguez, R., Pérez, I., Martínez, I. (2011). Sensors for quality monitoring and control in the food industry. Alimentaria. 423, pp. 58-61.

[14] Kawano, S., Watanabe, H., Iwamoto, M. (1992). Determination of sugar content in intact peaches by near infrared spectroscopy with fiber optics in interactance mode. Journal of the Japanese Society for Horticultural Science. 61, pp. 445–451

[15] Kawano, S., Fujiwara, T., Iwamoto, M. (1993). Nondestructive determination of sugar content in satsuma mandarin using near infrared (NIR) transmittance. Journal of the Japanese Society for Horticultural Science. 62, pp. 465–470.

[16] Choi, C.H. (1998). Development of apple sorter by soluble solid content using photodiodes. Proceeding of Winter Conference of KSAM, Suwon. 3 (1), pp. 362–367.

[17] He, D.J., Maekawa, T., Morishima, H. (2001). Detecting device for on-line detection of internal quality of fruits using near infrared spectroscopy and the related experiments. Transactions of the Chinese Society of Agricultural Engineering. 17, pp. 146–148.

[18] Miller, W.M., Zude, M. (2002). NIR-based sensing coupled with physical/ color features to Identify Brix level of Florida citrus. ASAE Meeting, Paper Number: 026037.

[19] Salguero-Chaparro, L., Rodriguez, F.P. (2014). On-line versus off-line NIRS analysis of intact olives. LWT - Food Science and Technology, 56, pp 363-369.

[20] Matheyambath, A.C., Subramanian, J., Paliyath, G. (2016). Mangoes. Reference Module in Food Science. Encyclopedia of Food and Health. pp. 641-645.

[21] Rumainum, I. M., Worarad, K., Srilaong, V., Yamane, K. (2018). Fruit quality and antioxidant capacity of six Thai mango cultivars. Agriculture and Natural Resources. 52(2), pp. 208-214. doi:10.1016/j.anres.2018.06.007

[22] Thai fresh mango. Retrieved from https://www.tgfresh.com/product/thai-fresh-mango/ Accessed on (24 September, 2018)

[23] Njuguna, J.K. (2017). Evaluation of Mango (Mangifera Indica L.) Mineral Nutrition On Jelly Seed Disorder, Fruit Yeild and Quality. Master's thesis dissertation, University of Nairobi

[24] Padda, M. S., do Amarante, C. V. T., Garcia, R. M., Slaughter, D. C., Mitcham, E. J. (2011). Methods to analyze physico-chemical changes during mango ripening: A multivariate approach. Postharvest Biology and Technology. 62(3), pp 267–274. doi:10.1016/j.postharvbio.2011.06.002

[25] Sivakumar, D., Jiang, Y., & Yahia, E. M. (2011). Maintaining mango (Mangifera indica L.) fruit quality during the export chain. Food Research International. 44(5), pp 1254–1263. doi:10.1016/j.foodres.2010.11.022

[26] Subedi, P. P., Walsh, K. B., & Owens, G. (2007). Prediction of mango eating quality at harvest using short-wave near infrared spectrometry. Postharvest Biology and Technology, 43(3), pp 326–334. doi:10.1016/j.postharvbio.2006.09.012

[27] Ueda, M., Sasaki, K., Utsunomiya, N., Inaba, K, Shimabayashi, Y. (2000). Changes in Physical and Chemical Properties during Maturation of Mango Fruit (Mangifera indica L. "Irwin") Cultured in a Plastic Greenhouse. Food Science and Technology Research. 6(4), pp 299–305. doi:10.3136/fstr.6.299

[28] Kienzle, S., Sruamsiri, P., Carle, R., Sirisakulwat, S., Spreer, W., & Neidhart, S. (2011). Harvest maturity specification for mango fruit (Mangifera indica L. "Chok Anan") in regard to long supply chains. Postharvest Biology and Technology. 61(1), pp. 41–55. doi:10.1016/j.postharvbio.2011.01.015

[29] Marques, E. J. N., de Freitas, S. T., Pimentel, M. F., & Pasquini, C. (2016). Rapid and non-destructive determination of quality parameters in the "Tommy Atkins" mango using a novel handheld near infrared spectrometer. Food Chemistry. 197, pp 1207–1214. doi:10.1016/j.foodchem.2015.11.080

[30] Ngamchuachit, P., Sivertsen, H. K., Mitcham, E. J., Barrett, D. M. (2015). Influence of cultivar and ripeness stage at the time of fresh-cut processing on instrumental and sensory qualities of fresh-cut mangos. Postharvest Biology and Technology. 106, pp 11–20. doi:10.1016/j.postharvbio.2015.03.013.

[31] Beckles, D. M. (2012). Factors affecting the postharvest soluble solids and sugar content of tomato (Solanum lycopersicum L.) fruit. Postharvest Biology and Technology, 63(1), 129–140. doi:10.1016/j.postharvbio.2011.05.016

[32] Schmilovitch, Z., Mizrach, A., Hoffman, A., Egozi, H., Fuchs, Y. (2000). Determination of Mango physiological indices by near- infrared spectrometry. Postharvest Biology and Technology. 19, pp 245–252.

[33] Delwiche, S. R., Mekwatanakarn, W., & Wang, C. Y. (2008). Soluble solids and simple sugars measurement in intact mango using near infrared spectroscopy. Horticulture Technology. pp 18(3), 410-416.

[34] Liu, F.-X., Fu, S.-F., Bi, X.-F., Chen, F., Liao, X.-J., Hu, X.-S., & Wu, J.-H. (2013). Physico-chemical and antioxidant properties of four mango (Mangifera indica L.) cultivars in China. Food Chemistry. 138(1), pp 396–405. doi:10.1016/j.foodchem.2012.09.111

[35] Jha, S. N., Kingsly, A. R. P., Chopra, S. (2006). Physical and mechanical properties of mango during growth and storage for determination of maturity. Journal of Food Engineering. 72(1), pp 73–76. doi:10.1016/j.jfoodeng.2004.11.020

[36] Bradley, R. L. (2010). Moisture and Total Solids Analysis. In Nielsen, S.S (Eds), Food Analysis. Springer, Boston, USA. 85–104. doi:10.1007/978-1-4419-1478-1_6

[37] Nyasordzi, J., Friedman, H., Schmilovitch, Z., Ignat, T., Weksler, A., Rot, I., Lurie, S., (2013). Utilizing the IAD index to determine internal quality attributes of apples at harvest and after storage. Postharvest Biology. Technology. 77, pp 80–86.

[38] McDonald, H., Arpaia, M.L., Caporaso, F., Obenland, D., Were, L., Rakovski, C., Prakash, A. (2013). Effect of gamma irradiation treatment at phytosanitary dose levels on the quality of 'Lane Late' navel oranges. Postharvest Biology. Technology. 86, pp 91–99

[39] Wei, Z., Wang, J. (2013). The evaluation of sugar content and firmness of nonclimacteric pears based on voltammetric electronic tongue. Journal of Food Engineering. 117, 158–164

[40] Magwaza, L. S., Opara, U. L. (2015). Analytical methods for determination of sugars and sweetness of horticultural products—A review. Scientia Horticulturae. 184, pp 179–192. doi:10.1016/j.scienta.2015.01.001

[41] Nor, F.M., Ismail, A.K., Clarkson, M., Othman, H. (2014). An improved ring method for calibration of hydrometers. Measurement 48, pp 1–5.

[42] Siesler, H.W. (2002). Introduction. In SieslerH.W, Ozaki, Y., Kawata, S., Heise, H.M. (Eds), Near-Infrered Spectroscopy: Principles, Instrument, Application. Wiley-VCH, Verlag, Germany.

[43] Sandorfy, C.R., Buchet, C.R., Lachenal, G. (2007). Principles of Molecular Vibrations for Near-Infrared Spectroscopy. In Ozaki, Y., McClure, F., Christy, A.A. (Eds), Near Infrared in Food Science and Technology. Wiley Interscience, Hoboken, New Jersey

[44] Williams, P. (2007). Near Infrared Technology – Getting the Best out of Light. Short course in the practical implementation of Near Infrared Spectroscopy for the user. PDK Grain, Nanaimo, British Columbia, and Winnipeg, Manitabo Canada.

[45] Osborne, B.G., Fearn, T., Hindle, P.H. (1993). Practical NIR Spectroscopy with Applications in Food and Beverage Analysis. Longman Scientific & Technical.

[46] Siesler, H.W. (2007). Basic Principles of Near-Infrared Spectroscopy. In Burns, P.A and Ciurczak, E.W (Eds) Handbook of Near Infrared Analysis third edition. CRC Press, Taylor and Francis Group, New York, Boca Raton.

[47] Larkin, P. (2011). Infrared and Ramen Spectroscopy: Principle and Spectral Interpretation. Elsevier, 225 Wyman Street, Waltham, MA 02451, USA.

[48] Miller, C.E. (2001). Chemical principle of Near Infrared Technology. In Williams, P and Norris, K. (Eds) Near Infrared Technology in the Agriculture and Food Industry. American Society of Cereal Chemists, Inc. St. Paul, Minnisota, USA.

[49] Aenugu, H. P. R., Kumar, D. S., Srisudharson, N. P., Ghosh, S. S., & Banji, D. (2011). Near infra red spectroscopy–an overview. International Journal of Chem Tech Research. 3(2), pp 825-836.

[50] Abbas, O., Baetan, V. 2018. Near Infrared Spectroscopy. In Franca, A.S. and Nollet, L.M.L (Eds), Spectroscopic Methods in Food Analysis. CRC Press, Taylor & Francis Group, New York, Boca Raton, USA.

[51] McCarthy, W.J., Kemeny, G.J. (2007). Fourier Transform Spectrophotometers in the Near-Infrared. In Burns, P.A and Ciurczak, E.W (Eds) Handbook of Near Infrared Analysis third edition. CRC Press, Taylor and Francis Group, New York, Boca Raton.

[52] Application note AN N283. 2018. Why FT-NIR Spectroscopy? [Online] Available: https://www.bruker.com/fileadmin/user_upload/8-PDF Docs/OpticalSpectrospcopy/FT-NIR/AN_N283_Why_FT-NIR_Spectrocopy_EN.pdf

[53] Bates J.B. (1978). Fourier Transform Spectroscopy. Computer and Mathematics with Application, 4(2), 73-84.

[54] Metrohm A.G. (2013). Monograph: A guide to near-infrared spectroscopic analysis of industrial manufacturing processes. [Online] Available: https://www.metrohm.com/en-th/documents/81085026

[55] Pasikatan, M. C., Steele, J. L., Spillman, C. K., Haque, E. (2001). Near Infrared Reflectance Spectroscopy for Online Particle Size Analysis of Powders and Ground Materials. Journal of Near Infrared Spectroscopy. 9(3), pp 153–164. doi:10.1255/jnirs.303

[56] Hildrum, K.I., Nilsen, B.N., Westad, F., Wahlgren, N.M. (2004). In-Line Analysis of Ground Beef Using a Diode Array near Infrared Instrument on a Conveyor Belt. Journal of Near Infrared Spectroscopy, 12(6), 367–376. doi:10.1255/jnirs.445

[57] Choi H. "Advantages of Photo diode Array." [Online] Available: http://www.hwe.oita-u.ac.jp/kiki/ronnbunn/paper_choi.pdf. Assessed on 24 September 2018.

[58] Osborne, B.G. (2000). Near-infrared spectroscopy in food analysis. In: Meyers, R.A. (Ed.), Encyclopedia of Analytical Chemistry. John Wiley & Sons Ltd, pp. 1–13.

[59] Wetzel, D.L.B. (1998). Analytical near infrared spectroscopy. In: Wetzel, D.L.B., Charalambous, G. (Eds.), Instrumental Methods in Food and Beverage Analysis. Elsevier, Amsterdam, pp. 141–194.

[60] Kortum, G. (1969). Reflectance Spectroscopy: Principles, Methods, Applications. Berlin: Springer Verlag.

[61] Davies, A.M.C., Grant, A. (1987). Review: Near infra-red analysis of food. International Journal of Food Science and Technology. 22(3), pp 191–207. doi:10.1111/j.1365-2621.1987.tb00479.x

[62] Kawata, S. (2002). New Techniques in Near Infrared Spectroscopy. In Siesler, H.W., Ozaki, Y., Kawata S., Heise, H.M. Near Infrared Spectroscopy Principles, Instruments, Applications. Wiley-VCH, Weinheim (Germany), pp 75-85.

[63] Malinen, J., Känsäkoski, M., Rikola, R., Eddison, C. G. (1998). LED-based NIR spectrometer module for hand-held and process analyser applications. Sensors

and Actuators B: Chemical. 51(1-3), pp 220–226. doi:10.1016/s0925-4005(98)00198-1

[64] Stark, E., Luchter, K. (2005). NIR Instrumentation Technology. NIR News.16(7), pp 13–16. doi:10.1255/nirn.855

[65] Palmer, C. A., Loewen, E. G. (2005). Diffraction Grating Handbook. New York, N.Y.: Newport Corp.

[66] Xie, L.J., Wang., Xu, H.R., Fu, X.P., Ying, Y.B. (2016). Applications of Near-Infrared Systems for Quality Evaluation of Fruits: A Review. Transactions of the ASABE. 59(2), pp 399–419. doi:10.13031/trans.59.10655

[67] Macclure W.F., Tsuchikawa S. (2007). Instrument. In Ozaki, Y., McClure, W.F., Christy, A.A (eds). Near Infrared in Food Science and Technology. Wiley Interscience. Hoboken, New Jersey, USA.

[68] Lajunen L.H.J. (1992). Spectrochemical analysis by atomic absorption and emission. Cambridge Royal Society of Chemistry.

[69] Sila, A. M. (2016). Multivariate calibration techniques for Infrared Spectroscopy data. Doctoral dissertation, School of Mathematics, University of Nairobi.

[70] Bhu, D. Chemometric Analysis for Spectroscopy. https://www.camo.com/downloads/resources/application_notes/Chemometric%20Analysis%20for%20Spectroscopy.pdf (Accessed date September 10, 2018).

[71] Hruschka, W.R. (2001). Data Analysis: Wavelength selection Methods. In Williams, P and Norris, K. (Eds) Near Infrared Technology in the Agriculture and Food Industry. American Society of Cereal Chemists, Inc. St. Paul, Minnisota, USA.

[72] Conzen, J.P. (2006). Multivariate Calibration: A practical guide for developing methods in the quantitative analytical chemistry. 2nd ed. Germany: Bruker Optik GmbH.

[73] Rinnan A., van den Berg F., Engelsen S.B. 2009. Review of the most common preprocessing techniques for near infrared spectra. Trend in Analytical Chemistry. 28, pp 1201-1222.

[74] CAMO. “The Unscramble Appendices: Method Reference.” [Online] Available: http://www.camo.com/Theunscrambler/Appendices. Accessed on September, 25 2018.

[75] Buddenbaum, H., Steffens, M. (2012). The Effects of Spectral Pretreatments on Chemometric Analyses of Soil Profiles Using Laboratory Imaging Spectroscopy. Applied and Environmental Soil Science. pp 1–12. doi:10.1155/2012/274903

[76] Barnes, R. J., Dhanoa, M. S., & Lister, S. J. (1989). Standard normal variate transformation and de-trending of near-infrared diffuse reflectance spectra. Applied spectroscopy. 43(5), pp. 772-777.

[77] Sanchez, J. (1991). Martens, Harald; Naes, Tormod: Multivariate Calibration. John Wiley & Sons, Chichester 1989, 419+ xvii pp., ISBN 0471 90979 3. Biometrical Journal, 33(4), pp 418-418.

[78] Næs, T., Isaksson, T., Fearn, T., Davies, T. (2002). A user-friendly guide to Multivariate Calibration and Classification. NIR Publication, Chichester, U.K.

[79] Andrade-Garda J.M., Boque-Marti R., Ferre-Baldrisch J., Carlosena-Zubieta A. (2009) Partial least square regression. In J. M Andrade-Garda (eds) Basic Chemometric Technique in atomic spectroscopy. Cambridge: Royal Society of Chemistry, pp. 181-243.

[80] Geladi P. and Kowalski B.R. (1986). Partial Least Square Regression: a tutorial. Analytica Chemica Acta. 85, pp. 1-17.

[81] Romia M.B and Bernardez M.C. (2009). Multivariate Calibration for Quantitative Analysis. In Sun D.A. Infrared Spectroscopy for Food Quality Analysis and Control. Amsterdam: Elsevier, pp. 51-82.

[82] Shrestha, A. (2016). Feasibility study on Near Infrared Spectroscopy for evaluation of combustion performance parameters and moisture content of Bamboo Chips. Master Dissertation, King Mongkut's Institute of Technology Ladkrabang.

[83] Williams, P.C. (2001). Implementation of Near-Infrared Technology. In Williams, P and Norris, K. (Eds) Near Infrared Technology in the Agriculture and Food Industry. American Society of Cereal Chemists, Inc. St. Paul, Minnisota, USA.

[84] Reich, G. (2005). Near-infrared spectroscopy and imaging: Basic principles and pharmaceutical applications. Advanced Drug Delivery Reviews. 57(8), pp. 1109-1143.

[85] Salguero-Chaparro, L., Baeten, V., Abbas, O., Rodriguez, F.P. 2012. On-line analysis of intact olive fruits by Vis-NIR Spectroscopy: Optimization of the acquisition parameters. Journal of Food Engineering. 112, pp. 152-157.

[86] Rodriguez-Saona, L. E., Fry, F. S., McLaughlin, M. A., Calvey, E. M. (2001). Rapid analysis of sugars in fruit juices by FT-NIR spectroscopy. Carbohydrate Research, 336(1), pp. 63–74. doi:10.1016/s0008-6215(01)00244-0

[87] Liu, Y., Ying, Y. 2005. Use of FT-NIR spectrometry in non-invasive measurements of internal quality of 'Fuji' apples. Postharvest Biology and Technology. 37, pp. 65–71.

[88] Ying, Y.B., Liu, Y.D., Wang, J.P., Fu, X.P., Li, Y.B. 2005. Fourier transform near-infrared determination of total soluble solids and available acid in intact peaches. Trans. ASAE. 48, pp. 229–234.

[89] Nicola¨ı, B.M., Verlinden, B.E., Desmet, M., Saevels, S., Theron, K., Cubeddu, R., Pifferi, A., Torricelli, A., 2007. Time-resolved and continuous wave NIR reflectance spectroscopy to predict firmness and soluble solids content of Conference pears.

Postharvest Biology and Technology. 47(1) pp. 68-74. doi:10.1016/j.postharvbio.2007.06.001, in press.

[90] Fan, G., Zha, J., Du, R., Gao, L. (2009). Determination of soluble solids and firmness of apples by Vis/NIR transmittance. Journal of Food Engineering. 93(4), pp. 416–420. doi:10.1016/j.jfoodeng.2009.02.006

[91] Maertens, K., Reyns, P., De Baerdemaeker, J. (2004). On-line measurement of grain quality with NIR technology. Transactions of the ASAE. 47(4), pp. 1135–1140. doi:10.13031/2013.16545

[92] Posom, J., Sirisomboon, P. (2017). Evaluation of the higher heating value, volatile matter, fixed carbon and ash content of ground bamboo using near infrared spectroscopy. Journal of Near Infrared Spectroscopy. 25(5), pp. 301–310.

[93] Abbott, J. A., Lu, R., Upchurch, B. L., Stroshine, R.L. (1997). Technologies for non-destructive quality evaluation of fruits and vegetables. In Horticultural reviews — Technologies for nondestructive quality evaluation of fruits and vegetables, 20, 1–120. John Wiley & Sons, Inc.

[94] Zanobini, A., Sereni, B., Catelani, M., Ciani, L. (2016). Repeatability and reproducibility techniques for the analysis of measurement systems. Measurement. 86, pp. 125-132.

[95] Sharma, S., and Sirisomboon, P. (2017). Precision Test for Spectral Characteristic of On-line Vis-NIR versus At-line NIR Spectroscopy for Measuring Total Soluble Solids of Mango (Mangifera indica CV Nam Doc Mai). 10th TSAE International Conference, TSAE 2017.

[96] Berntsson, O., Danielsson, L. G., & Folestad, S. (2001). Characterization of diffuse reflectance fiber probe sampling on moving solids using a Fourier transform near-infrared spectrometer. Analytica chimica acta, 431(1), pp. 125-131.

[97] Dardenne, P. (2010). Some considerations about NIR spectroscopy: Closing speech at NIR-2009. NIR news. 21(1), pp. 8-14.

[98] Nordey, T., Joas, J., Davrieux, F., Chillet, M., Léchaudel, M. (2017). Robust NIRS models for non-destructive prediction of mango internal quality. Scientia Horticulturae, 216, 51-57.

[99] Marques, E. J. N., de Freitas, S. T., Pimentel, M. F., & Pasquini, C. (2016). Rapid and non-destructive determination of quality parameters in the 'Tommy Atkins' mango using a novel handheld near infrared spectrometer. Food chemistry, 197, pp. 1207-1214.

[100] Rungpichayapichet, P., Mahayothee, B., Nagle, M., Khuwijitjaru, P., Müller, J. (2016). Robust NIRS models for non-destructive prediction of postharvest fruit ripeness and quality in mango. Postharvest Biology and Technology. 111, pp. 31-40.

[101] Schmilovitch, Z. E., Mizrach, A., Hoffman, A., Egozi, H., Fuchs, Y. (2000). Determination of mango physiological indices by near-infrared spectrometry. Postharvest biology and technology. 19(3), pp. 245-252.

[102] Golic, M., Walsh, K., Lawson, P. (2003). Short-wavelength near-infrared spectra of sucrose, glucose, and fructose with respect to sugar concentration and temperature. Applied spectroscopy. 57(2), pp. 139-145.

Total Soluble Solids (TSS) measured by reference method used for model development.

Sample	TSS value for Atline scanning	TSS value for Online scanning
1A	17.7	18.2
1B	18.0	18.1
2A	19.5	19.0
2B	19.0	18.9
3A	18.1	18.5
3B	14.7	15.2
4A	15.6	16.5
4B	16.6	17.0
5A	19.2	18.5
5B	18.5	18.9
6A	20.1	19.6
6B	18.3	18.2
7A	17.8	18.1
7B	18.4	18.5
8A	16.8	16.7
8B	16.9	17.4
9A	16.7	17.4
9B	17.8	17.8
10A	16.8	17.0
10B	17.4	17.8
11A	18.5	18.7
11B	18.5	18.3
12A	18.9	18.8
12B	18.9	19.0
13A	17.8	18.0
13B	17.8	18.1
14A	18.6	18.8
14B	18.8	19.1
15A	16.4	16.9
15B	17.3	17.4
16A	16.5	16.8
16B	18.4	17.1
17A	16.6	16.4
17B	18.8	18.7

18A	18.0	18.5
18B	16.6	16.6
19A	16.1	16.5
19B	16.5	16.5
20A	15.3	15.4
20B	16.4	16.4
21A	18.6	18.5
21B	16.4	16.6
22A	15.8	16.4
22B	17.6	18.2
23A	18.3	18.7
23B	17.7	18.1
24A	16.5	17.0
24B	17.2	17.2
25A	16.8	17.4
25B	16.4	16.2
26A	17.6	17.8
26B	17.9	17.2
27A	18.2	17.9
27B	17.7	17.6
28A	18.1	17.6
29B	16.0	15.9
30A	16.6	16.7
30B	17.7	17.9
31A	17.5	18.2
31B	17.5	17.5
32A	16.7	16.9
32B	17.6	18.0
33A	17.3	17.7
33B	17.7	17.2
34A	17.1	16.6
34B	16.1	16.7
35A	17.9	17.5
35B	17.7	17.9
36A	16.6	16.5
36B	16.6	17.0
37A	17.0	16.9

37B	15.7	15.5
38A	15.0	15.7
38B	15.2	15.4
39A	14.7	15.4
39B	17.7	17.9
40A	17.2	18.1
40B	16.8	17.5
41A	15.7	17.0
41B	14.2	14.4
42A	15.4	15.3
42B	15.0	15.6
43A	15.7	16.3
43B	16.3	16.9
44A	16.3	16.2
44B	15.5	15.5
45A	15.9	16.2
45B	16.0	16.7
46A	15.4	15.7
46B	15.7	16.1
47A	16.3	16.5
47B	17.2	17.5
54A	14.0	14.1
54B	17.8	17.6
55A	17.4	17.9
55B	15.6	15.7
56A	17.6	17.3
56B	17.2	17.1
57A	17.8	17.8
57B	16.3	17.2
58A	15.7	16.6
58B	14.4	15.1
59A	15.0	15.6
59B	15.5	16.6
60A	16.4	17.2
60B	15.2	15.2
61A	15.0	15.3
61B	15.4	15.8

62A	16.0	16.3
62B	13.9	15.6
63A	14.5	14.5
64B	16.9	16.6
65A	14.1	15.1
65B	15.8	15.8
66A	16.4	16.7
66B	15.8	16.2
67A	16.4	17.2
67B	16.6	17.0
68A	15.9	16.1
68B	16.4	16.9
69A	15.5	16.0
69B	17.7	17.4
70A	19.9	19.3
70B	18.9	19.4
71A	17.3	18.1
71B	17.3	17.2
72A	18.0	18.3
72B	17.2	18.1
73A	16.0	16.5
73B	18.4	18.1
74A	18.0	18.2
74B	15.5	16.4
75A	17.0	16.8
75B	16.1	15.5
76A	15.8	16.3
76B	18.8	19.6
77A	19.3	19.8
77B	18.2	18.2
78A	17.9	18.0
78B	19.1	18.8
79A	18.6	17.9
79B	16.9	17.3
80A	16.4	16.8
80B	17.5	17.3
81A	16.4	16.7

81B	17.2	17.0
82A	16.6	16.9
82B	16.6	16.8
83A	16.2	16.0
83B	19.2	18.6
84A	17.4	17.8
84B	17.2	17.6
85A	18.0	18.5
85B	15.0	15.1
86A	14.9	14.8
86B	16.2	16.8
87A	17.8	17.5
87B	16.4	16.9
88A	17.1	16.8
88B	16.1	16.6
89A	15.6	16.8
89B	16.4	17.2
90A	16.2	16.7
90B	15.2	15.4
91A	15.7	15.8
91B	16.0	16.8
92A	16.6	17.4
92B	16.9	17.0
93A	15.5	15.7
93B	15.3	15.5
94A	17.5	17.9
94B	15.4	15.6
95A	16.3	16.7
95B	17.3	17.7
96A	14.8	14.9
96B	15.0	15.5
97A	15.1	15.6
97B	14.8	15.3
98A	15.4	15.3
98B	15.9	16.1
99A	18.1	18.0
100A	17.3	18.2

Total Soluble Solids (TSS) measured and predicted for unknown sample set using offline condition.

SAMPLE	MEASURED TSS (%BIRX)	PREDICTED TSS (%BRIX)
1	18.3	16.2
2	19	17.0
3	18.4	17.5
4	17.9	16.8
5	18.7	18.2
6	19.7	18.3
7	18.9	18.2
8	18.3	17.3
9	16.8	17.1
10	18	15.4
11	17.8	16.4
12	18.4	15.6
13	17	15.8
14	19.7	17.8
15	16.5	16.5
16	19.5	15.3
17	17.2	15.0
18	16.4	15.9
19	17.9	17.3
20	16.8	16.5
21	15.4	15.5
22	19.3	17.7
23	18.2	16.1
24	16.5	15.2
25	17.2	15.3
26	17.5	14.7
27	17.1	15.1
28	16.9	14.0
29	19.5	17.7
30	15	13.9
31	17	16.5
32	17.6	15.7
33	16.5	15.2

34	16.6	14.9
35	17.4	14.6
36	17.4	15.8
37	15.5	13.9
38	16.2	15.5
39	18	16.1
40	19.1	16.7
41	17.3	16.2
42	18.4	16.6
43	17.6	16.3
44	16.4	14.6
45	17	15.0
46	16.5	14.5
47	18.6	17.2
48	17.9	16.0
49	17	14.9
50	18.5	16.6
51	16.1	14.9
52	15.2	13.6
53	17.7	16.6
54	18.8	15.9
55	18.5	16.3
56	18	16.3
57	18.5	16.3
58	18.3	15.2
59	16.5	15.5
60	18.2	15.3
61	19.4	16.8
62	17.6	15.4
63	18.3	17.5
64	16.9	14.9
65	18.7	16.4
66	19	17.0
67	20.1	17.4
68	18.4	17.7
69	18.2	18.2
70	18.3	16.7

71	19.5	17.7
72	19.6	18.1
73	17.4	16.6
74	19.1	15.7
75	19.5	17.7
76	19.6	17.4
77	19	17.3
78	19.8	19.1
79	18.9	16.8
80	19.2	16.3
81	18.3	16.3
82	19	17.2
83	20.1	16.7
84	18.6	17.4
85	16.8	16.3
86	18.2	17.4
87	17.4	15.2
88	19	17.5
89	19.3	18.0
90	19.1	17.3
91	19.5	17.7
92	18.7	17.4
93	17.5	16.8
94	17.9	16.0
95	17.5	17.7
96	20.1	15.8
97	18.5	16.0
98	16.3	14.6
99	16.2	16.5
100	16.3	16.3
101	16.3	16.3
102	17.5	16.7
103	18.7	19.2
104	15.1	16.3
105	19.3	17.0
106	15.9	15.6

Total Soluble Solids (TSS) measured and predicted for unknown sample set using online condition.

SAMPLE	MEASURED TSS (%BRIX)	PREDICTED TSS (%BRIX)
1	18.4	16.4
2	19.1	18.6
3	18.6	16.7
4	18.4	17.2
5	19.0	17.3
6	19.4	17.4
7	18.0	17.2
8	17.9	16.8
9	18.6	17.0
10	18.6	17.6
11	18.5	16.8
12	17.5	16.4
13	19.5	17.3
14	17.1	15.5
15	19.6	18.0
16	17.4	17.1
17	16.7	16.7
18	18.1	18.0
19	17.1	18.1
20	15.8	16.6
21	19.5	18.9
22	18.5	18.1
23	16.9	17.9
24	17.2	18.5
25	17.7	18.2
26	17.7	18.6
27	16.9	17.5
28	19.6	18.9
29	15.1	16.4

30	16.9	17.7
31	17.9	17.1
32	17.0	16.8
33	16.5	16.5
34	17.6	16.9
35	17.5	15.3
36	15.5	15.5
37	16.0	16.1
38	18.3	16.5
39	19.1	17.9
40	17.1	18.3
41	18.5	17.0
42	18.0	18.7
43	16.5	16.4
44	17.8	17.2
45	16.6	16.1
46	18.9	19.2
47	18.0	18.6
48	17.4	15.1
49	18.8	17.7
50	16.3	17.4
51	15.4	15.5
52	18.9	16.5
53	18.9	17.6
54	18.2	17.9
55	18.6	16.0
56	18.8	17.9
57	18.8	17.2
58	17.3	16.4
59	18.6	16.5
60	19.5	17.8
61	18.3	17.4

62	19.0	18.7
63	16.9	15.9
64	19.3	17.1
65	18.9	16.5
66	19.0	17.1
67	18.2	17.8
68	18.6	18.1
69	19.8	17.7
70	17.8	17.3
71	19.4	16.9
72	19.2	19.2
73	18.9	18.7
74	19.2	17.0
75	19.2	16.7
76	17.1	16.3
77	18.5	16.8
78	18.2	16.0
79	19.8	14.7
80	19.7	16.7
81	19.5	17.2
82	19.1	16.7
83	17.3	15.8
84	18.3	14.6
85	18.3	16.6
86	18.6	17.1
87	17.1	14.5
88	16.8	15.3
89	16.9	14.5
90	17.5	15.3
91	18.7	16.6
92	19.0	16.2
93	14.9	15.0

94	19.7	16.5
95	15.7	16.1

การประชุมวิชาการสมาคมวิศวกรรมเกษตรแห่งประเทศไทยระดับชาติ ครั้งที่ 18 และระดับนานาชาติ ครั้งที่ 10 ประจำปี 2560
The 18th TSAE National Conference and the 10th TSAE International Conference : TSAE 2017

FE006

Precision Test for Spectral Characteristic of On-line Vis-NIR versus At-line NIR Spectroscopy for Measuring Total Soluble Solids of Mango (*Mangifera indica* CV Nam Doc Mai)

Sneha Sharma[1]*, Panmanas Sirisomboon[1]

[1]Department of Agricultural Engineering, Faculty of Engineering, King Mongkut's Institute of Technology Ladkrabang, Bangkok 10520, Thailand.

Corresponding author: Sneha Sharma. E-mail: sharmasneha0725@gmail.com

Abstract

Near Infrared (NIR) Spectroscopy is known as a rapid technique to evaluate the quality traits of fruits and vegetables. Precision and accuracy of the instrument is an important aspect in order to obtain results with minimum error. The main objective of this paper is to determine scanning repeatability and reproducibility of UV-VIS-NIR spectrometer (on-line) and NIR spectrometer (at-line) for measuring total soluble solids of Mango (*Mangifera indica* CV Nam Doc Mai) and its corresponding reference method using digital refractometer. Results shows that the repeatability and reproducibility of on-line scanning spectrometer is 0.01071 and 0.023393, similarly for at-line scanning spectrometer with 0.000775 and 0.008262 respectively. Maximum co-efficient of determination R^2_{MAX} of reference method is 0.967. This result could be beneficial for the development of model using on-line or at-line spectrometer.

Keywords: Precision test, Spectral characteristic, On-line, At-line, Total Soluble Solids, Mango.

1. Introduction

Mango (*Mangifera indica*) is one of the favorite fruit worldwide. It has several variety with different specifications, one of the common variety is Nam Doc Mai. This variety of mango is consumed widely and is most preferable because of its good taste and appearance. During the ripening process, the mango fruit becomes softer and there are several physiochemical changes that undergoes during different stages. There is an increase in the soluble sugars content known as total soluble solids, TSS as the ripening stage of mango increases. Total soluble solids is one of the parameters for quality assessment in mango fruit (Schmilovitch et al., 2000).

In order to evaluate the quality traits of Mango fruit Near Infrared (NIR) spectroscopy is known as a rapid and accurate technique. Many researches related to the methods for implementation of NIR spectroscopy has been successfully published and some are ongoing. There are several advantage of NIR spectroscopy compared to some traditional chemical methods like fast speed, accuracy, minimal sample preparation, no use of chemical, fast processing and result etc. Despite of these advantages, limited work has been able to publish in the field of on-line monitoring by NIR spectroscopy in industrial plant (Salguero-Chaparro et al., 2012).

Same variety of mango may have different shape, size, color, taste etc even when they are harvested at the same time. It is now important for the cultivars to know the difference among the same variety of fruits and sort them on the basis of their quality. Conventional methods for the determination of quality parameters are very time consuming and labor intensive (Huang et al., 2008). Many research has shown the robustness of the model in laboratory condition (off-line/ at-line) but online monitoring condition for quality analysis is more desirable nowadays. Despite these studies, the acquisition of spectral data from a moving sample (for instance, during an on-line process, on a conveyor belt or through a pipe), is quite complex (Andersson et al., 2005). The on-line acquisition of a spectrum from a moving sample is dependent on many different parameters such as physical nature of the material (particle size, shape, orientation and density) as well as the type and the composition of the material (Fernandez-Ahumada, 2008).

In order to develop a robust model based on online and at-line scanning the precision test of the instrument as well as the referencing laboratory is most important.

Repeatability and reproducibility are the parameters that describe the precision of scanning. The main aim of this paper is to test for scanning repeatability and reproducibility as well as reference method repeatability.

2. Materials and Methods

2.1 Sample Preparation.

For the experiment Mango cv. Nam doc mai sample were brought from Chachangsao province on June 3, 2017. From the samples 3 mango are selected for precison test in NIRS Research Centre of Agriculture Product and Food (www.nirsresearch.com), Department of Agricultural Engineering, Faculty of Engineering, King Mongkut's Institute of Technology Ladkrabang, Thailand.

2.2 At-line Scanning

Samples were scanned by using NIR Multi-Purpose Analyzer (MPA) Spectrometer (Bruker optics, Germany) with scanning resolution of 16cm^{-1} in absorbance mode and there were 32 scans for 1 average spectrum of the sample. Before sample scanning the gold plate was scanned as a background. Wavenumber was from 12,500-4,000 nm.

2.3 On-line Scanning

On-line scanning was done by UV-Vis-NIR Spectrometer, AvaSpec-2048 – USB2 standard fiber optic spectrometer, wavelength from 200-1160 nm with integration time of 7 ms and focal length of 2.5mm approximately depend on the fruit size. For on-line scanning, sample was placed in a conveyor belt inside a black box in which the Avaspec fibre optic was mounted from the top.

2.4 Repeatability and reproducibility of scanning test.

For repeatability test each samples were loaded and scanned 10 times in same position for both at-line and on-line process. Similarly for reproducibility samples were reloaded and rescanned for 9 times.

2.5 Reference method

After scanning samples were brought for reference laboratory. Samples were cut into halves and total soluble solids of the sample was measured using Digital Hand-held "Pocket" Refractometer PAL-1 S/No L218454, Atago Japan.

2.6 Repeatability for reference method.

Repeatability of reference method can be defined as the standard deviation of difference between the repeat measurements. In this experiment, one slice of Mango is divided into three parts to measure total soluble solids and each part has three repeat measurements.

3. Result and Discussion

To obtain scanning repeatability and reproducibility for at-line scanning three wavelengths were selected. Wavenumber 10306 cm^{-1} (970nm) i.e band of water, 6943 cm^{-1} (1440 nm) i.e band of sucrose and 6326 cm^{-1} (1580 nm) band of starch were selected (Figure 1). Standard deviation of the absorbance value at the selected wavelength gives the repeatability and reproducibility of NIR instrument on sample. For measurement of repeatability and reproducibility for on-line scanning wavelength selected are 760 nm i.e band of water, 680 nm i.e band of chlorophyll, 913 nm i.e band of sucrose (Figure. 2).

Table 1 Repeatability and reproducibility by on-line and at-line scanning.

Scanning	Repeatability	Reproducibility
On-line	0.01071	0.023393
At-line	0.000775	0.008262

From table 1 we can observe that the repeatability and reproducibility of at-line scanning is low, 0.000775 and 0.008262. Repeatability gives the variation between the measurements of different sample by using same device under same operating condition. Reproducibility gives the dispersion of result under different condition. In this experiment reproducibility is calculated by varying the orientation of Mango during scanning. Low repeatability value means low variation between the measurements that indicate highly repeatable and precise scanning instrument. More robust model can be expected form at-line scanning instrument.

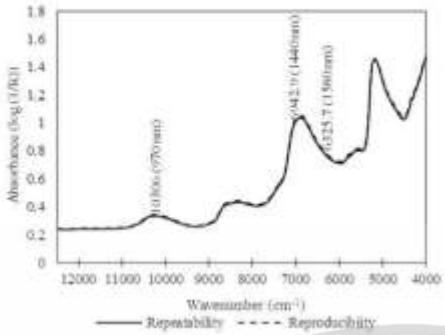

Figure.1 Average Spectra from At-line Scanning

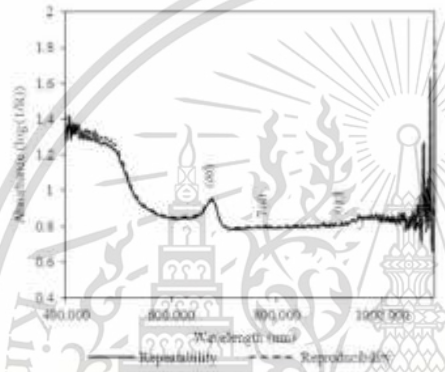

Figure2 Average Spectra from On-line Scanning

However, there are many source of error that can occur in on-line scanning process. The surface roughness of the sample, the average distance from the sample to the optics are parameters that can also significantly influence the quality, repeatability and reproducibility of the spectra generated (Berntsson et al., 2001). In order to obtain robust models for NIR spectroscopy applications with an acceptable level of accuracy and precision, it is essential to set up the optimal operational conditions to assess the adequate online measurement (Salguero-Chaparro et al., 2012).

According to Dardenne (2010) for reference laboratory, the maximum coefficient of determination, R^2_{Max} is calculated using formula;

$$R^2_{Max} = \frac{SD_y^2 - REP^2}{SD_y^2} \quad (1)$$

Where, SD_y is the standard deviation of the measured value of total soluble solids and REP is the repeatability of the reference data. Repeatability of reference data is calculated (0.1403). R^2_{Max} was obtained to be 0.967 that means it is possible to develop NIR model using total soluble solids reference method. R^2_{Max} is possible only when there is no error in the spectra or model (Dardenne, 2010). It depends on the range and precision of reference data. The error from reference method was 3.3%.

4. Conclusions

From this experiment, we observed that on-line and at-line scanning instrument can be used to make a model. Compared to on-line scanning, at-line scanning gave more precise and accurate result. Precision analysis for reference laboratory indicates that good model can be developed using total soluble solids of Mango.

5. Acknowledgements

The author would like to acknowledge NIRS Research Centre of Agriculture Product and Food (www.nirsre-search.com), Department of Agricultural Engineering, Faculty of Engineering, King Mongkut's Institute of Technology Ladkrabang, Thailand for providinging me the space and the instrument during the experiment and would also like to acknowledge King Mongkut's Institute of Technology Ladkrabang, Thailand for providing Foreign Student Research Fund.

6. References

Andresson, M., Svensson, O., Folestad, S., Josefson, M., Wahlund, K.G. 2005. NIR spectroscopy on moving solids using a scanning grating spectrometer—impact on multivariate process analysis. Chemometrics and Intelligent Laboratory Systems 75, 1-11.

Berntsson, O., Danielsson, L.G., Folestad, S., 2001. Characterization of diffuse reflectance fiber probe sampling on moving solids using a Fourier transform near-infrared spectrometer. Analytica Chimica Acta 431, 125–131

Dardenne, P. 2010. Some consideration about NIR spectroscopy: Closing speech at NIR – 2009. NIR news 21(1), 8-14.

Fernandez- Ahumada, E. 2008. Assessment of the potential of Near Infrared Reflectance Spectroscopy to be

implemented in the feed manufacturing industry for process control. PhD Thesis. University of Cordoba

Huang, H., Yu, H., Xu, H., Ying, Y. 2008. Near Infrared Spectroscopy for On/In line monitoring of quality in food and beverages: A review. Journal of Food Engineering, 87(3), 303-313.

Salguero-Chaparro, L., Baeten, V., Abbas, O., Rodriguez, F.P. 2012. On-line analysis of intact olive fruits by Vis-NIR Spectroscopy: Optimization of the acquisition parameters. Journal of Food Engineering 112, 152-157.

Schmilovitch, Z., Mizrach, A., Hoffman, A., Egozi, H., Fuchs, Y. 2000. Determination of mango physiological indices by near-infrared spectrometry. Postharvest Biology and Technology 19, 245–252.

Author biography

Name-Surname	Sneha Sharma
Date of birth	10 November 1993
Current address	KMITL Condominium 08, Chalongkrung road, Ladkrabang, Bangkok.
Permanent address	Bhairahawa, Rupendehi, Nepal
Email address	sharmasnehe0725@gmail.com
Contact number	062-850-5253
Education background	Master of Engineering (Agricultural Engineering), 2018 King Mongkut's Institute of Technology Ladkrabang Ladkrabang, Bangkok, Thailand Bachelor in Mechanical Engineering, 2015 Kathmandu University Kavre, Dhulikhel, Nepal
Conferences	Sharma S., and Sirisomboon P. " Precision Test for Spectral Characteristic of On-line Vis-NIR versus At-line NIR Spectroscopy for Measuring Total Soluble Solids of Mango (Mangifera Indica CV Nam Doc Mai)." The 18th Thai Society of Agricultural Engineering International Conference and 10th Thai Society of Agricultural Engineering International Conference (TSAE2017), Thailand (2017), Pp. 45-48.